Metabolic Engineering 70 (2022) 166–180

Contents lists available at ScienceDirect

Metabolic Engineering

journal homepage: www.elsevier.com/locate/meteng

A manipulation of carotenoid metabolism influence biomass partitioning and fitness in tomato

Jianing Mi [a], Jose G. Vallarino [b], Ivan Petřík [c], Ondřej Novák [c], Sandra M. Correa [b], Monika Chodasiewicz [a,b], Michel Havaux [d], Manuel Rodriguez-Concepcion [e], Salim Al-Babili [a], Alisdair R. Fernie [b], Aleksandra Skirycz [b,f], Juan C. Moreno [a,b,*]

[a] Center for Desert Agriculture, Biological and Environmental Science and Engineering Division (BESE), King Abdullah University of Science and Technology (KAUST), Thuwal, Saudi Arabia
[b] Max Planck Institut für Molekulare Pflanzenphysiologie, Am Mühlenberg1 D-14476, Potsdam-Golm, Germany
[c] Laboratory of Growth Regulators, Faculty of Science, Palacký University and Institute of Experimental Botany, The Czech Academy of Sciences, Šlechtitelů 27, CZ-78371, Olomouc, Czech Republic
[d] Aix-Marseille University, CEA, CNRS UMR7265, BIAM, CEA/Cadarache, F-13108 Saint-Paul-lez-Durance, France
[e] Institute for Plant Molecular and Cell Biology (IBMCP) UPV-CSIC, 46022, Valencia, Spain
[f] Boyce Thompson Institute, Cornell University, Ithaca, NY, United States

ARTICLE INFO

Keywords:
Abiotic stress tolerance
Apocarotenoids
Biomass and yield
Carotenoids
Metabolic engineering
Metabolites and lipids
Phytohormones

ABSTRACT

Improving yield, nutritional value and tolerance to abiotic stress are major targets of current breeding and biotechnological approaches that aim at increasing crop production and ensuring food security. Metabolic engineering of carotenoids, the precursor of vitamin-A and plant hormones that regulate plant growth and response to adverse growth conditions, has been mainly focusing on provitamin A biofortification or the production of high-value carotenoids. Here, we show that the introduction of a single gene of the carotenoid biosynthetic pathway in different tomato cultivars induced profound metabolic alterations in carotenoid, apocarotenoid and phytohormones pathways. Alterations in isoprenoid- (abscisic acid, gibberellins, cytokinins) and non-isoprenoid (auxin and jasmonic acid) derived hormones together with enhanced xanthophyll content influenced biomass partitioning and abiotic stress tolerance (high light, salt, and drought), and it caused an up to 77% fruit yield increase and enhanced fruit's provitamin A content. In addition, metabolic and hormonal changes led to accumulation of key primary metabolites (e.g. osmoprotectants and antiaging agents) contributing with enhanced abiotic stress tolerance and fruit shelf life. Our findings pave the way for developing a new generation of crops that combine high productivity and increased nutritional value with the capability to cope with climate change-related environmental challenges.

1. Introduction

Climate change and the increasing world population are serious challenges facing agriculture and food security (Pareek et al., 2020). Indeed, current estimates indicate that food production should be doubled by 2050 (Ort et al., 2015; Xu, 2016). However, global warming and the anthropogenic activities that affect agricultural ecosystems and subsequent crop yield render this doubling a very difficult goal to achieve. Moreover, abiotic stresses, especially salinity and drought, cause considerable crop losses, with yield reductions of almost 50% (Hussain et al., 2019; Roy et al., 2014). Therefore, a new generation of crops with enhanced fitness—as exemplified, for instance, by simultaneously improved photosynthetic efficiency, stress tolerance, and yield—are urgently needed to meet the desired levels of crop productivity. In the past decade, photosynthesis and photorespiration have been the preferred targets for manipulation to improve plant yield (Ding et al., 2016; Lopez-Calcagno et al., 2019; Simkin et al., 2015, 2017; South et al., 2019; Timm et al., 2015). Two breakthrough genetic strategies for crop improvement, which are based on manipulating the xanthophyll cycle and glycolate metabolism, were reported to lead to a 15% and 37%

Abbreviations: ABA, Abscisic acid; GA, Gibberellins; β-cc, β-cyclocitral; Zaxinone, Zax; SLs, Strigolactones; LCYB, Lycopeneβ-cyclase; JA, Jasmonic acid.

* Corresponding author. Max Planck Institut für Molekulare Pflanzenphysiologie, Am Mühlenberg1 D-14476, Potsdam-Golm, Germany.
E-mail address: juancamilo.morenobeltran@KAUST.edu.sa (J.C. Moreno).

https://doi.org/10.1016/j.ymben.2022.01.004
Received 13 August 2021; Received in revised form 29 December 2021; Accepted 9 January 2022
Available online 11 January 2022

biomass increase in the cash crop tobacco (Kromdijk et al., 2016; South et al., 2019). However, neither of these strategies have been demonstrated to work in food crops. Moreover, manipulation of the xanthophyll cycle in Arabidopsis resulted in a contradictory reduction in plant biomass (Garcia-Molina and Leister, 2020), bringing into question the general applicability of this method.

Another possibility for increasing plant yield and fitness in crops might be provided by manipulating the content of carotenoids (e.g., β-carotene), which are isoprenoid pigments that rank among the most important plant secondary metabolites due to the diverse functions they fulfil in photosynthesis and signaling. Within chloroplasts, carotenoids, such as β-carotene and xanthophylls, are key components of photosynthetic membranes and form pigment-protein complexes that are essential for photoprotection (Niyogi and Truong, 2013; Xu et al., 2020). β-Carotene is also the precursor of abscisic acid (ABA) and strigolactones (SLs). Hence, alterations in carotenoid content can affect hormone homeostasis and subsequently plant development and physiology (Al-Babili and Bouwmeester, 2015; Nambara and Marion-Poll, 2005). Recently, new signaling and growth-promoting functions have been reported for further carotenoid-derived molecules (i.e. apocarotenoids), including β-cyclocitral (β-cc), and zaxinone (Zax) (D'Alessandro et al., 2018; D'Alessandro et al., 2019; Dickinson et al., 2019; Hou et al., 2016; Moreno et al., 2021b; Wang et al., 2019). In animals, carotenoids consumed in the diet are cleaved to produce retinoids, including vitamin A, and are important antioxidants protecting from several age related diseases, such as macular degeneration (Rodriguez-Concepcion et al., 2018). β-Carotene is the main precursor of vitamin A in animals and the main precursor of several apocarotenoids and plant hormones in plants; therefore, increased accumulation of β-carotene might indirectly influence plant growth and development, as well as improve the nutritional value. β-Carotene is produced by the action of lycopene β-cyclase (LCYB), indicating a potential for genetic manipulation of the expression of this gene as a two-for-one solution to improve both the fitness and the nutritional value of the chosen crop.

In our previous work, we expressed the carrot (*Daucus carota*) *DcLCYB1* gene in tobacco and demonstrated growth-promoting and developmental effects of this gene (Moreno et al., 2016, 2020). Interestingly, these tobacco lines also showed enhanced tolerance to abiotic stresses, in addition to enhanced biomass, yield, and photosynthetic efficiency (Moreno et al., 2021a). These beneficial effects were likely triggered by an enhanced accumulation of the phytohormones ABA and gibberellins (GA), but they were also a result of the greater photoprotection afforded by the accumulation of xanthophylls. We therefore hypothesized that any LCYB-encoding gene, independent of its origin (plant or bacterial), might led to beneficial effects similar to those observed with the *DcLCYB1* gene in tobacco (Moreno et al., 2020). To evaluate this hypothesis and considering that manipulation of carotenoid content may increase the nutritional value of tomato fruits, we analyzed previously generated tomato lines that overexpress one of three different *LCYB* genes (from plant and bacterial origins) following plastid or nuclear transformation. Despite some gene-dependent specific differences between the lines, we confirmed that the overexpression of any of these *LCYB* genes is sufficient to trigger a molecular response that results in increased pro-vitamin A and a modulated hormone profile, accompanied by alterations in plant growth and architecture, and abiotic stress tolerance.

2. Methods

2.1. Plant material and growth conditions

Tomato wild type (*S. lycopersicum* cvs. IPA6+/lutein, IPA6-/without lutein and isogenic Red Setter/R.S.), transplastomic (pNLyc#2 and LCe), and nuclear (high carotenoid/H.C.) lines (Apel and Bock, 2009; D'Ambrosio et al., 2004; Wurbs et al., 2007) were raised from seeds germinated on soil. The transgenic lines harbor *LCYB* genes from daffodil, tomato, and bacteria (*Erwinia uredovora*). Two of the selected lines were obtained by plastid DNA transformation (pNLyc#2 and LCe) and the other line by Agrobacterium-mediated nuclear DNA transformation (H. C.; Table S1). Transplastomic lines expressing the *LCYB* gene from daffodil or *Erwinia uredovora* (pNLyc#2 and LCe, respectively) were generated using particle bombardment. The homoplasmic state (i.e., the absence of residual copies of the wild-type genome) of ~22 plants was assessed by subjecting the transgenic plants to double-resistance tests (spectinomycin and streptomycin, 500 mg l^{-1}) on synthetic media and by RFLP (Apel and Bock, 2009; Wurbs et al., 2007). Due to the homoplasmic state (meaning that plastid DNA was equally modified in all chloroplasts of the transgenic lines) and to the similar phenotype observed in these lines, we selected one line per genotype (T3 generation of pNLyc#2 and LCe lines) to carry out the experiments described in this work. The H.C. nuclear line (plus other six LCYB transgenic lines) was obtained via *Agrobacterium* transformation. All seven transgenic lines expressing the tomato *LCYB* were confirmed by Southern blot experiments and by the orange color in their fruit in comparison to the isogenic R.S. control. In addition, northern blot and qPCR experiments confirmed higher transcript accumulations in the transgenic lines in leaves and fruit than in the isogenic R.S. control (D'Ambrosio et al., 2004; Giorio et al., 2007). Based on this evidence and the similar phenotype obtained in all nuclear lines, we selected the H.C. line (T5 generation) with the highest β-carotene levels for the experiments in this work.

Wild type and transgenic lines were grown side by side, and randomly allocated, in the greenhouse (semi-controlled conditions) under standard conditions (16 h/8 h day/night regime, 450–800 μmol photons m^{-2} s^{-1} combination of artificial light and sunlight, 24 °C, and 65% relative humidity). Plant height, leaf and fruit number, internode length, and seed yield were recorded. Fully expanded mature source leaves (the 5th leaf) were harvested from six-week-old wild type and transgenic *LCYB* tomato plants ($n = 5$) grown in the greenhouse. Fruits were analyzed as five biological replicates from 16-week-old tomato plants. Each biological replicate consisted of a pool of three different fruits from one individual plant.

2.2. Biomass quantification

Wild type and transgenic lines were grown directly on soil. Plants were grown for three weeks in a controlled environment (100–250 μmol m^{-2} s^{-1}, 23 °C) and then transferred to fully controlled (plant chamber/530 and 53 μmol m^{-2} s^{-1} red and white light respectively, 16/8 h photoperiod, 70% relative humidity and 24 °C), semi-controlled (greenhouse/average light intensity: 170–380 μmol m^{-2} s^{-1}, maximum light intensity: 1200 μmol $m^{-2}s^{-1}$ and 24 °C), and uncontrolled conditions (polytunnel/natural climate conditions during spring-summer 2019 in Potsdam, Germany). In each climate condition, plants were grown side by side and they were randomly distributed with at least 50 cm of space between each other. Physiological parameters, such as plant height and leaf and fruit number, were recorded through development (10–60–70 days of growth under the different climate conditions) and/or before performing the biomass experiment. Plant biomass for plants grown in fully controlled conditions was assessed in 11-week-old plants (only the biomass of the aerial part, leaf and stem, was recorded). Plant (leaves and stem) and fruit biomass for plants grown under semi-controlled conditions was assessed in two groups of 8- and 16-week-old plants, respectively. The first group was grown for quantification of the leaves and stem ($n = 5$–6), and the second was grown for the assessment of fruit biomass ($n = 5$). Both groups were grown in parallel and harvested at different time points (eight and 16 weeks, respectively). The biomass of plants grown under uncontrolled conditions in the polytunnel was measured in 12-week-old tomato plants. In this case, the leaf, stem and fruit biomass was recorded from the same plants. Briefly, leaves, stem, and fruit were separated and the fresh weight was recorded immediately. Subsequently, the leaves, stem, and fruit were dried at 70 °C for five days, and the dry weight was recorded. Five

(biomass) to ten (plant height) biological replicates were used for each experiment under the different climate conditions. For fruit size quantification, the area of three fully ripened fruit detached from three different greenhouse-grown 16-week-old tomato plants was quantified using ImageJ software.

2.3. Photosynthesis measurements

Wild type and transgenic lines were raised from seeds and grown for three weeks under fully controlled conditions in a phytotron (250 μmol photons m^{-2} s^{-1}, 16 h/8 h day/night, 22 °C day/18 °C night, 70% relative humidity; pots of 7 cm diameter). The plants were then transferred to the greenhouse (16 h/8 h day/night regime, 450–800 μmol photons m^{-2} s^{-1} combination of artificial and sun light, 24 °C, 65% relative humidity), randomly allocated, and acclimated for four weeks before the photosynthetic measurements (49-day-old plants). Photosynthetic parameters, such as CO_2 assimilation, conductance, and relative electron transport rate (rETR), were measured with a Li-6400XT portable photosynthesis system equipped with a leaf chamber fluorometer (Li-Cor Inc., Lincoln, NE, USA). The measurements were performed during the mornings on fully expanded leaves under growth light conditions (greenhouse, 450 μmol (photons) $m^{-2}s^{-1}$ of PAR), with the amount of blue light set at 10% of the photosynthetically active photon flux density to optimize stomatal aperture. The reference CO_2 concentration was set at 400 μmol CO_2 mol^{-1} air. All measurements were performed using a 2 cm^2 leaf chamber maintained with a block temperature of 25 °C and a flow rate of 300 mmol air min^{-1}. The rETR was calculated according to the method described in (Krall and Edwards, 1992). In addition, total non-photochemical quenching (NPQT), (ΦPSII), (ΦNPQ), and (ΦNO) were measured in the same plants with a MultiSpec (Photosync) instrument (Kuhlgert et al., 2016; Tietz et al., 2017). All measurements were conducted during the early morning (9:00–11:00 a.m.) in the same part of the 7th leaf from seven-week-old plants ($n = 5$–12).

2.4. Water deficit and salinity treatments

Water deficit and salinity treatments were performed under greenhouse conditions. Tomato seeds were sown and raised under control conditions in a phytotron. After three weeks, the seedlings were transferred to the greenhouse and acclimated for four days. The plants were randomized and placed 30 cm apart. For water deficit experiments ($n = 5$-6), control plants were watered once per day (50–200 mL per plant, depending of their water requirements), whereas stressed plants were not watered. Plant height was recorded before the stress treatment was initiated (day 0) and again at day 10 of the stress conditions. Phenotypes were recorded by photography at the same time points. For salinity stress ($n = 5$-6), plants were watered with 100 mL of water or 100 mL salt solution (NaCl 200 mM) once per day for seven days. Plant height was recorded at day 0 before the onset of the stress treatment and seven days later. At day seven, the stress treatment was discontinued and all plants were watered with 100 mL water for one more week. The plants were photographed again at two weeks after the stress onset (one week of salt treatment and a subsequent week of water only).

2.5. Photooxidative stress

Leaf discs (1.2 cm diameter) were floated on water at 10 °C and simultaneously exposed for 18 h to strong white light (photon flux density/PFD, 1200 mmol photons m^{-2} s^{-1}) produced by an array of light-emitting diodes. The stressed leaf discs were then placed on wet filter paper for measurement of autoluminescence emission after a 2 h dark adaptation, as previously described (Birtic et al., 2011). The emission signal was imaged with a liquid nitrogen-cooled charge--coupled device (CCD) camera (VersArray 1300B, Roper Scientific), with the sensor operating at a temperature of −110 °C. The acquisition time was 20 min, and on-CCD 2 × 2 binning was used, leading to a resolution of 650 × 670 pixels. As previously shown, the imaged signal principally emanates from the slow decomposition of the lipid peroxides that accumulated in the samples during the oxidative stress treatment (Birtic et al., 2011).

2.6. Shelf-life experiments

Tomato fruits ($n = 5$) were harvested from 16-week-old wild type and transgenic lines and kept for seven weeks at 23 °C and a relative humidity ~20%. The fruit phenotype was recorded 0, 8, 16, 24, 32, 40, and 48 days after detachment from the plant.

2.7. Microscopy analysis

Fully ripened tomato fruits were detached from 12-week-old tomato plants for further microscopy analysis. Lycopene and β-carotene (Lyc+β-car; laser excitation of 488 nm and emission between 400 and 550 nm) were observed with a Leica DM6000B/SP5 confocal laser-scanning microscope (Leica Microsystems, Wetzlar, Germany), following a previously published protocol (D'Andrea et al., 2014). The total fluorescence of the generated micrographs was quantified using the ROI function in Fiji software, based on collected data from three different tomato fruits from each line.

2.8. HPLC analysis of pigments

Plastid isoprenoids (chlorophylls, carotenoids, and tocopherols) were extracted and quantified as described previously (Emiliani et al., 2018).

2.9. Profiling of tomato apocarotenoids using UHPLC-QQQ-MS/MS

Analysis of tomato apocarotenoids was performed on a Vanquish™ Flex UHPLC System with an ACQUITY UPLC BEH C18 column (100 × 2.1 mm, 1.7 μm, Waters) coupled with a Triple Quadrupole Mass Spectrometer (TSQ Altis™, Thermo Scientific) with a heated-electrospray ionization source. Briefly, approximately 25 mg tomato tissue powder spiked with internal standards (IS) mixture (including D_3-β-ionone, D_3-β-apo-11-carotenal, D_3-3-OH-β-apo-13-carotenone, D_3-β-apo-13-carotenone, D_3-β-apo-15-carotenal, D_3-β-apo-14'-carotenal, D_3-β-apo-12'-carotenal, D_3-β-apo-10'-carotenal, and D_3-β-apo-8'-carotenal; 2.5 ng each standard) was extracted with methanol containing 0.1% butylated hydroxytoluene twice in an ultrasound bath, followed by the centrifugation. The supernatant was collected and dried under vacuum. The residue was re-dissolved in 150 μL of acetonitrile/water (90:10, v:v) and filtered through a 0.22 mm filter for UHPLC-MS analysis (Mi et al., 2018). Apocarotenoid profiling was performed by using UHPLC-QQQ-MS/MS in selective reaction monitoring (SRM) mode. The MS parameters were 3.5 KV of spray voltage, 40 Arb of sheath gas, 10 Arb of Aux gas, 325 °C of ion transfer tube temperature, 275 °C vaporizer temperature, and 1.0 mTorr of CID gas. The SRM transition list is shown in Table S6 (Kössler et al., 2021). Apocarotenoid standards (Buchem B.V., Apeldoorn, Netherlands) including β-cyclocitral, 3-OH-β-ionone, β-ionone, 3-OH-β-apo-11-carotenal, β-apo-11-carotenal, 3-OH-β-apo-13-carotenone, β-apo-13-carotenone, 3-OH-β-apo-15-carotenal, β-apo-15-carotenal, β-apo-14'-carotenal, 3-OH-β-apo-12'-carotenal, β-apo-12'-carotenal, 3-OH-β-apo-10'-carotenal, β-apo-10'-carotenal, 3-OH-β-apo-8'-carotenal, β-apo-8'-carotenal were used to validate the identification of apocarotenoids from tomato using UHPLC-QQQ-MS/MS.

2.10. Hormone quantification/hormonomics

Levels of endogenous phytohormones (cytokinins, auxins, jasmonates, abscisates, gibberellins, and salicylic acid) were determined in

five biological replicates of freeze-dried tomato leaves and fruit, according to a modified method described previously (Simura et al., 2018). Briefly, samples containing 1 mg DW of biological material were extracted in an aqueous solution of 50% acetonitrile (v/v). A mixture of stable isotope-labeled standards of phytohormones was added to validate the LC-MS/MS method. Crude extracts were loaded onto conditioned Oasis HLB columns (30 mg/1 ml, Waters) and washed with 30% aqueous acetonitrile. Flow-through fractions containing purified analytes were collected and evaporated to dryness in a vacuum evaporator. The chromatographic separation was performed using an Acquity I class system (Waters, Milford, MA, USA) equipped with an Acquity UPLC® CSH C18 RP column (150 × 2.1 mm, 1.7 μm; Waters). The eluted compounds were analyzed using a triple quadrupole mass spectrometer (Xevo™ TQ-XS, Waters) equipped with an electrospray ionization source. Data were processed with Target Lynx V4.2 software, and final concentration levels of phytohormones were calculated by isotope dilution (Rittenberg and Foster, 1940). List of hormones and intermediates is available in Table S2.

2.11. Profiling of gibberellins by using UHPLC-QQQ-MS/MS

Levels of endogenous gibberellins (GAs) were determined in five biological replicates of freeze-dried tomato leaves and fruit using UHPLC-QQQ-MS/MS. Briefly, approximate 15 mg of tomato tissue powder spiked with 2 ng deuterium labeled gibberellins (internal standards, including D_2-GA1, D_2-GA3, D_2-GA4, D_2-GA9, and D_2-GA12, OlChemIm), were extracted with 0.5 mL of methanol in an ultrasound bath (Branson 3510 ultrasonic bath) for 15 min. After 8 min centrifugation at 14000 rpm at 4 °C, the supernatant was collected and the pellet was extracted twice with 0.2 mL of methanol. Next, the two supernatants were combined and dried under vacuum. The residue was re-dissolved in 50 μL of methanol, followed by a dilution with 1 mL of water, and loaded onto a GracePure™ C_{18}-Max SPE column (100 mg/1 mL) preconditioned with 1 mL of methanol and 2 mL of water. After being washed with 1 mL of water, GAs-enriched fraction was eluted in 1 mL of 50% aqueous acetonitrile and dried by nitrogen gas. The resulting GAs-enriched fraction was re-dissolved in 100 μL of 50% aqueous acetonitrile and filtered through a 0.22 μm filter before LC-MS analysis. Analysis of GAs was performed on a Vanquish™ Duo UHPLC Systems coupled with a TSQ Altis™ triple quadrupole mass spectrometer (Thermo Scientific) with a heated-electrospray ionization source. The chromatographic separation was carried out on an ACQUITY UPLC HSS T3 column (2.1 × 100 mm, 1.8 μm, Waters) and a VanGuard pre-column (2.1 × 5 mm, 1.8 μm, Waters) maintained at 40 °C. Mobile phases consist of 5% aqueous acetonitrile (A) and acetonitrile (B), both containing 0.01% formic acid. Both were employed for eluting GAs with the gradient program: 0–12 min, 5% B to 80% B; 12–13 min, 80% B to 100% B; 13–16 min, 100% B at 0.4 mL/min of flow rate. The MS parameters were as follows: negative ion, 3000 V; sheath gas, 45 Arb; aux gas, 10 Arb; sweep gas, 1 Arb; ion transfer tube temperature, 325 °C; vaporizer temperature, 300 °C; cycle time, 1 s; Q1 resolution (FWHM), 0.7; Q3 resolution (FWHM), 0.7; CID gas (mTorr), 1.5; and chromatographic peak width (sec), 6. The SRM transitions of gibberellins detected from tomato tissues are shown in Table S3. Data were processed with Xcalibur software (Thermo Scientific), and final concentration levels of GAs were calculated by internal standards.

2.12. Metabolite profile analysis

The methyl *tert*-butyl ether (MTBE) extraction buffer was prepared and samples extracted as described by Salem et al. (2016). For metabolites, the chromatograms and mass spectra were evaluated using ChromaTOF 1.0 (Leco, www.leco.com) and TagFinder v.4 (Luedemann et al., 2008). software, respectively. The mass spectra were cross-referenced using the Golm Metabolome database (Kopka et al., 2005). Data are reported following the standards (Dataset S1 and S2) suggested by Fernie et al. (2011).

2.13. Lipid profile analysis

After MTBE extraction, the lipid-containing fraction was dried, resuspended, and analyzed by LC-MS. Samples were run in negative and positive mode (Datasets S3 and S4). The mass spectra were processed with the Refiner MS 7.5 (Genedata) and Xcalibur software.

2.14. Statistical analyses

Statistical analysis was performed using GraphPad Prism (version 5.0) or R environment (version 3.5.2 https://www.R-project.org/). Growth and plant productivity were quantified by conducting a set of several experiments. First, growth curves for transgenic lines and their respective wild types were determined under fully controlled (plant chamber), semi-controlled (greenhouse), and uncontrolled (polytunnel/"field" experiment) conditions ($n = 10$). Physiological parameters (plant height, leaf number, fruit number) and plant productivity (fresh and dry matter of leaves, stems, and fruit) were quantified on plants grown under fully- ($n = 5$), semi- ($n = 5$–10), and uncontrolled conditions ($n = 5$–10). Fruit fresh and dry matter were quantified for the semi-controlled and uncontrolled conditions. Seed yield was quantified in an independent experiment as the total seed production of 12 transgenic and wild type plants for each genotype. Photosynthetic analysis was performed on plants grown under semi-controlled conditions ($n = 5$–12). Water deficit and salinity stress experiments were performed on three-week-old tomato plants grown under greenhouse conditions ($n = 5$–6). A non-paired two-tailed Student t-test was performed to compare each transgenic line with their respective wild type using GraphPad Prism software. Pigment, metabolite, lipid, and hormone quantifications were performed on tomato plants grown under semi-controlled conditions ($n = 5$–6). Pigments and hormones ($n = 5$) were analyzed with the unpaired two-tailed Student t-test to compare each transgenic line with their respective wild type (GraphPad Prism). For metabolomics ($n = 5$), data mining, normalization, clustering, and graphical representation were performed using R Software. For lipid analysis, the output data were normalized to the internal standard and the amount of dry sample used for the analysis (Datasets S5 and S6). For statistical analysis, the MetaboAnalyst webserver was used (Chong et al., 2019; Pang et al., 2020). The data were auto-scaled and normalized. The differences in the distribution of lipid profiles among the transgenic lines were visually explored by principal component analysis (PCA). The supervised partial least squares discriminant analysis (PLS-DA) was used when the separation obtained with PCA was inadequate. Significant differences were determined among the transgenic lines and their respective wild types with the non-parametric Wilcoxon rank-sum test ($n = 5$).

3. Results

3.1. Tomato productivity under different environmental conditions

Given our recent findings that expression of the carrot *DcLCYB1* gene in tobacco resulted in increased photosynthetic efficiency, photoprotection, stress tolerance, plant biomass, and yield (Moreno et al., 2020, 2021a), we decided to evaluate whether manipulation of LCYB activity could confer similar growth advantages in an economically important food crop. We tested our hypothesis by exploiting the availability of several tomato cultivars overexpressing different LCYB-encoding genes. In particular, we used a Red Setter cultivar with a nuclear construct overexpressing a tomato LCYB (line H.C.) and two transplastomic lines expressing LCYB-encoding genes from daffodil in the IPA6+ background (line pNLyc#2) or from the bacterium *Pantoea ananatis* (formerly named *Erwinia uredovora*) in the IPA6-background (line LCe) (Table S1). Growth evaluation under different climate conditions revealed robust and homogeneous changes in plant height

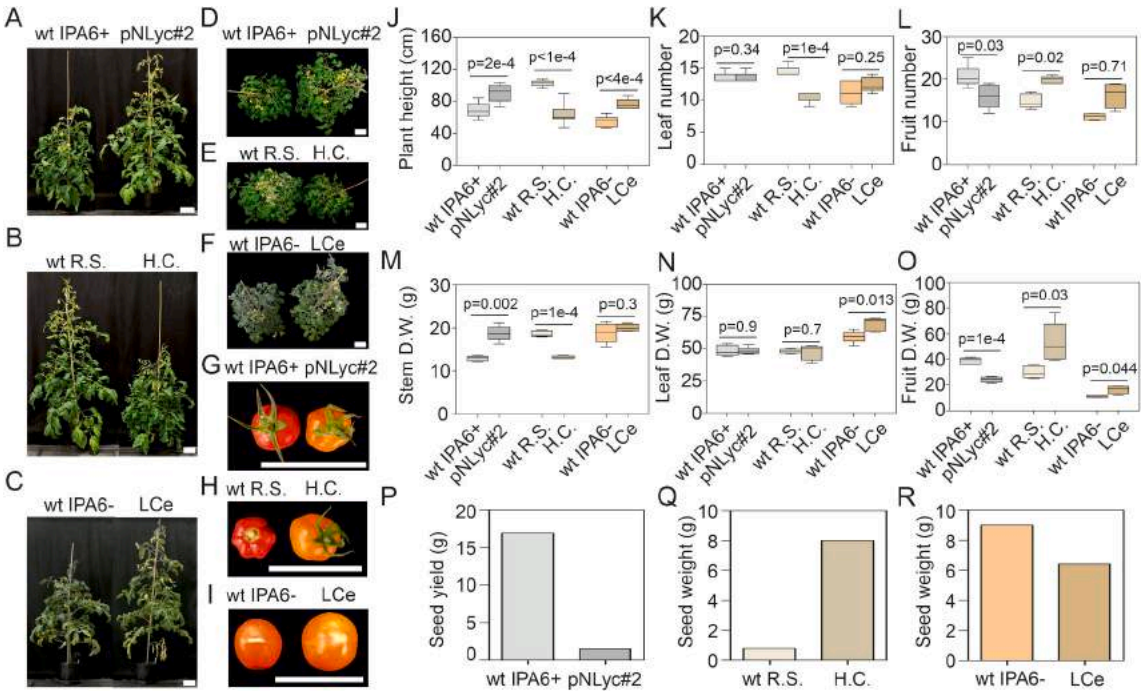

Fig. 1. Tomato plant yield under semi-controlled conditions in the greenhouse. (A–F) Nine-week-old wild type (IPA6+, R.S., and IPA6-) and transgenic tomato lines (pNLyc#2, H.C., and LCe) grown under greenhouse conditions. **(G–I)** Tomato fruits from 16-week-old wild type and transgenic tomato lines grown under greenhouse conditions (top view). **(J–O)** Plant height, leaf and fruit number, and dry weight biomass (leaf, stem, and fruit) of wild type and transgenic tomato lines (n = 5–10). **(P–R)** Seed yield of wild type and transgenic tomato lines grown under greenhouse conditions. Seed production was measured as the total weight of seeds produced by 12 independent tomato plants of each genotype. Unpaired two-tailed Student t-test was performed to compare transgenic lines with the wild type. wt: wild type; R. S.: Red Setter; H.C.: high carotene; LCe: lycopene β-cyclase from *Erwinia*. Scale bar: 10 cm.

(increased and reduced plant height for transplastomic and nuclear lines, respectively) of the transgenic lines in comparison to their respective wild type (Fig. S1). Due to the robustness of the phenotypes, we selected the semi-controlled conditions (greenhouse) to perform a detailed molecular and physiological characterization of this phenomenon. Interestingly, the transplastomic lines showed longer stems than their respective wild-type plants, thereby allowing a more spaced allocation of their leaves along the stem. By contrast, the H.C. nuclear line showed reduced plant height (Fig. 1A–C). In addition, leaves from pNLyc#2 were larger than the IPA6+ leaves, while leaves from the H.C. line were smaller than those from its wild type R.S. (Fig. S2A, D). By contrast, leaves from the LCe line showed sizes similar to the wild type (Fig. S2G). The fruit size was similar to the wild type in the pNLyc#2 line but was slightly larger in the LCe line (Fig. S2J), while the fruit from the H.C. line were considerably larger when compared to those from its respective wild type (Fig. S2B, E, H, J). Interestingly, all *LCYB* transgenic lines showed different biomass partitioning when comparing leaves, stem, and fruit (Fig. 1M-O). The pNLyc#2 line showed a clear increase in plant height (~30%) and stem biomass (45%), but no changes in leaf biomass or leaf number (Fig. 1J, K M, N). In addition, fruit biomass (37%) and fruit number were reduced, although the fruit size observed in pNLyc#2 was similar to the wild type (Fig. 1L, O). By contrast, the H. C. line showed reduced plant height (40%) and stem biomass (30%), but no changes in leaf biomass despite its reduced leaf number (Fig. 1J, K, M, N). In addition, the H.C. fruit biomass was increased by 77% compared to the wild type R.S. (Fig. 1O), in line with the increased fruit number and size displayed by this genotype (Fig. 1H, L). The LCe line showed increased plant height (~20%) and leaf biomass (17%), but no significant changes in stem biomass (Fig. 1J, M, N). Its fruit biomass was increased up to 45% relative to the wild type IPA6- (Fig. 1O). In this line, the leaf and fruit number remained the same as in the wild type (Fig. 1K and L). Seed production in pNLyc#2 and LCe transplastomic lines was lower than in their wild types, while H.C. seed production was approximately 1000% higher than in its respective wild type (Fig. 1P-R). Biomass quantification in plants grown under controlled and uncontrolled conditions showed similar patterns of biomass redistribution (as in the greenhouse) in the different plant tissues (Figs. S3-S4), but also revealed delayed and accelerated development for the pNLyc#2 and H. C. lines, respectively, while the LCe line showed wild-type-like development (Figs. S4-S5).

3.2. *LCYB-overexpressing lines show different carotenoid profiles in leaves and fruit*

We sought further insights into the different biomass accumulation patterns in leaves and fruits in the transgenic lines by investigating carotenoid accumulation in both organs, since an altered carotenoid content might affect hormone content and, thereby, plant growth. Transgenic lines expressing plant *LCYB*s showed a reduction in total leaf carotenoid content, with strong decreases in lutein and a lesser decrease in neoxanthin, but strong increases in violaxanthin and zeaxanthin levels. In addition, the H.C. line displayed a slight reduction in β-carotene levels. By contrast, the total carotenoid content in the bacterial *LCYB*-expressing LCe line remained essentially the same as in the wild type, with some slight reductions in β-carotene and zeaxanthin levels in the leaves (Fig. 2A and Fig. S6A, C, E).

In the fruit, the total carotenoid content in the transplastomic pNLyc#2 and LCe lines was unchanged, while the total carotenoid content was reduced in the H.C. line. Transgenic lines expressing plant *LCYB*s showed a strong accumulation of fruit β-carotene and strong reductions in lycopene, lutein, and phytoene, while an increase in only β-carotene was observed for the LCe line (Fig. 2A and Fig. S6B, D, F). In addition, carotenoid-rich crystal structures were observed by confocal microscopy in the fruit of the transgenic lines (Fig. S7). The content of other isoprenoids, such as chlorophyll remain unchanged in the pNLyc#2 and H.C. lines (with the exception of a slight reduction in

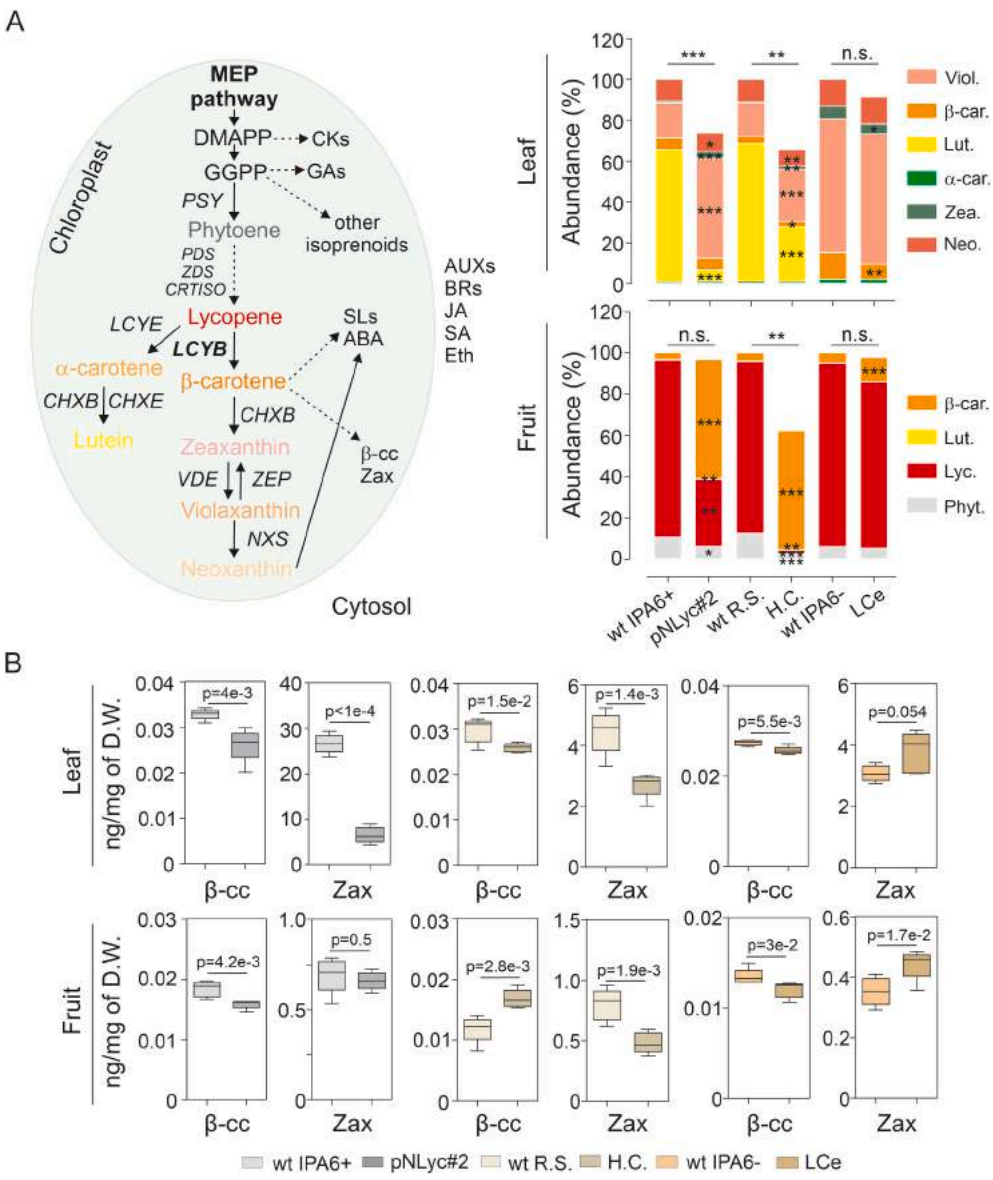

Fig. 2. Carotenoid and apocarotenoid metabolism in leaf and fruit of *LCYB*-expressing tomato lines. (A) Carotenoid pathway (left) and carotenoid composition (right) in leaves and fruits of wild type (IPA6+, R.S., and IPA6-) and *LCYB* transgenic lines (pNLyc#2, H.C., and LCe) grown in the greenhouse ($n = 5$). **(B)** Quantification of apocarotenoids with conserved growth-promoting properties (β-cyclocitral/β-cc and zaxinone/Zax) in leaves and fruits (see Figs. S11-15 for complete apocarotenoid profiling). Leaf samples were collected from the 5th leaf of six-week-old tomato plants. Fully ripened fruits were collected from 16-week-old tomato plants ($n = 5$; each biological replicate comprising a pool of 3 fruits). Unpaired two-tailed Student t-test was performed to compare transgenic lines with the wild type (*: $p < 0.05$, **: $p < 0.005$ ***: $p < 0.0005$). wt: wild type; R.S.: Red Setter; H.C.: high carotene; LCe: lycopene β-cyclase from *Erwinia*; DMAPP: dimethylallyl diphosphate; GGPP: geranylgeranyl diphosphate. Viol: violaxanthin; car: carotene; Zea: zeaxanthin; Neo: neoxanthin; Lyc: lycopene; Phyt: phytoene; Lut: lutein; ABA: abscisic acid; GAs: gibberellins; SLs: strigolactones; BRs: brassinosteroids; AUXs: auxins; CKs: citokinins; SA: salicylic acid; JA: jasmonic acid; Eth.: ethylene; PSY: phytoene synthase; PDS: phytoene desaturase; ZDS: z-carotene desaturase; CRTISO: carotene isomerase; CHX: carotenoid hydroxylase; VDE: violaxanthin de-epoxidase; ZEP: zeaxanthin epoxidase; NXS: neoxanthin synthase.

chlorophyll *b* in the H.C. line), while γ- and α-tocopherol contents were increased. The LCe line showed a reduction in α-tocopherol (Fig. S8). By contrast, the tocopherol content (α, δ, and γ-tocopherol) increased strongly in fruits of the pNLyc#2 line, while remaining unaltered in the H.C. and LCe lines (Fig. S8).

β-Carotene and xanthophylls are the main precursors of non-hydroxylated and hydroxylated apocarotenoids, respectively. Growth-promoting and signaling properties of some apocarotenoids (e.g., β-cyclocitral and zaxinone) have been reported in rice, tomato, and Arabidopsis (Dickinson et al., 2019; Wang et al., 2019). These previous findings and the altered pigment content observed in the leaves and fruits of the transgenic lines prompted us to profile apocarotenoid species in order to determine their contribution to the observed phenotypes (Fig. 2D and Fig. S12-15). In leaves, non-hydroxylated apocarotenoids showed few increases or wild-type-like levels (Fig. S12), in line with the wild-type-like β-carotene content in the transgenic lines. By contrast, hydroxylated apocarotenoids showed strong reductions due to a strong decrease in lutein content (Fig. S13). The non-hydroxylated apocarotenoids in fruit showed a strong and significant accumulation (due to enhanced β-carotene content; Fig. S14), while the hydroxylated apocarotenoids exhibited strong reductions due to the lower lutein content in the fruit (Fig. S15). Growth regulators, such as β-cc and Zax, were mainly found at reduced levels in the leaves and fruit (Fig. 2D). Other apocarotenoids with biological activity, such as β-ionone, showed enhanced accumulation in the fruit (Fig. S11).

3.3. Hormone metabolism is altered in LCYB-overexpressing lines

Altered β-carotene accumulation might influence the content of β-carotene-derived and/or isoprenoid-derived hormones (e.g., ABA and GAs, respectively), thereby influencing plant growth and development. We examined plant growth and development parameters (germination, primary root length, and biomass) known to be influenced by different phytohormones. Opposite to mature plants, 18-days old pNLyc#2 seedlings showed delayed radicle emergence and reduced growth, root length, and biomass, while the H.C. line showed higher radicle

emergence and cotyledon opening percentage, growth, and biomass compared to their wild types (Fig. 3A–E). Thus, suggesting an altered hormone composition. By contrast, the LCe line showed no significant changes in the parameters measured at this developmental stage when compared to its wild type (Fig. 3A–E). Next, we profiled the plant hormones to gain further insights into their contribution to the observed growth phenotype. The lines were characterized by significant increases in ABA and jasmonic acid (JA) for pNLyc#2; ABA reduction and IAA increments for H.C.; and ABA reduction and JA and JA-Ile increments in LCe in leaves (Fig. 3F). By contrast, stronger significant changes in hormone content were found in fruit. ABA, JA, and JA-Ile were increased, while indole acetic acid (IAA), the most bioactive auxin (Aux), was reduced in both the pNLyc#2 and H.C. lines but increased in the LCe line (Fig. 3F). In addition, SA was increased only in the pNLyc#2 line, whereas isopentenyladenine (iP), an active cytokinin (CK), was increased in the pNLyc#2 and LCe lines (Fig. 3F). Phaseic acid, a bioactive ABA catabolite, showed increased and reduced contents in the pNLyc#2 and H.C. lines, respectively. Intermediates of the ABA, GA, Aux, CKs, and JA metabolic pathways were also differentially affected in leaves and fruit (Fig. S9-10). Due to the low resolution of the technique to measure the content of the main GAs (GA_1, GA_3, GA_4), and considering these played a key role in the grow phenotype observed in *DcLCYB1* tobacco lines, we designed or own method (see Materials and Methods) to quantify the main GAs in leaves and fruits in our samples by using UHPLC-QQQ-MS/MS. GA_4 and GA_1, were enhanced in the leaves of transplastomic pNLyc#2 and LCe lines, while GA_3 was reduced in the

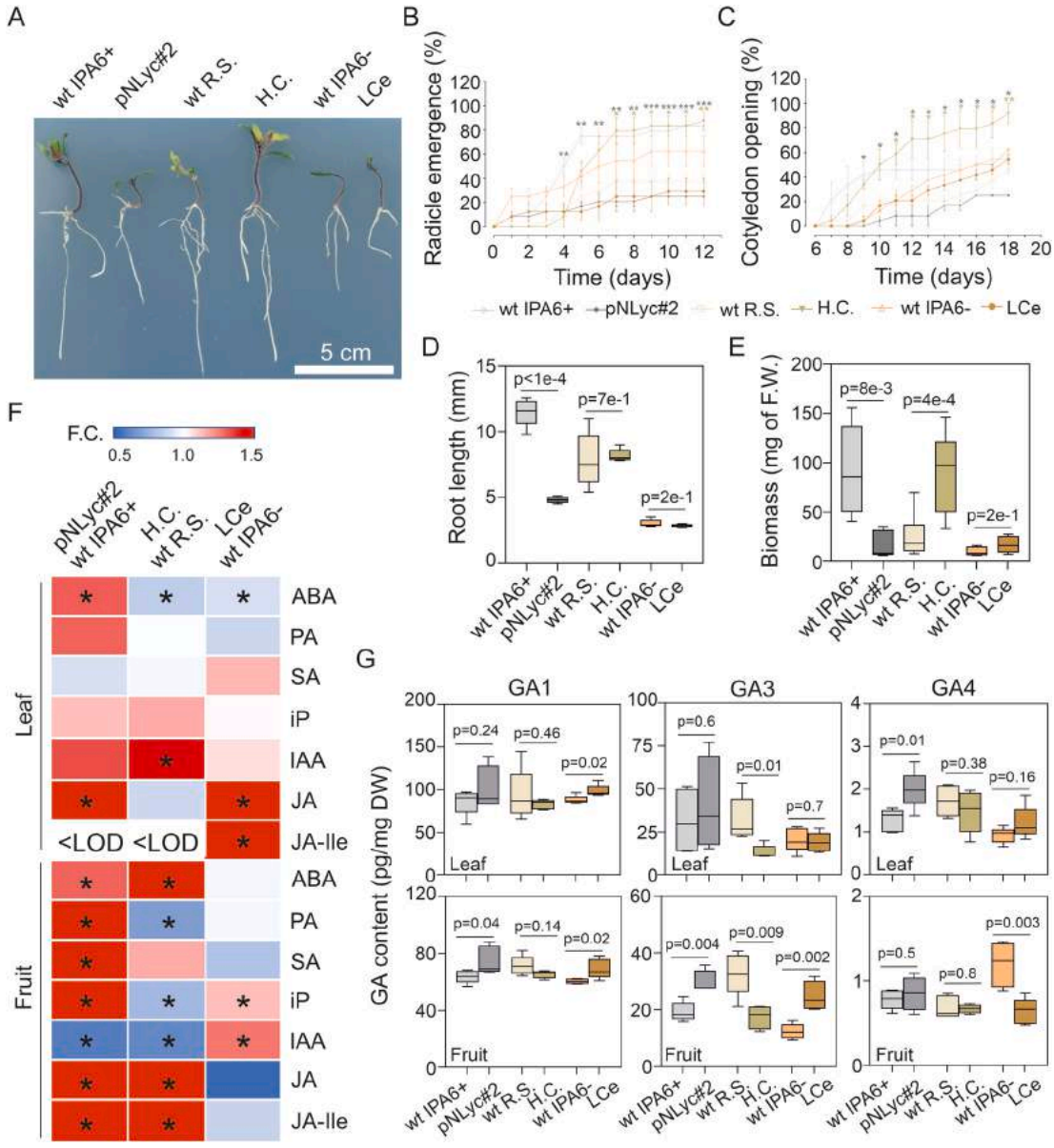

Fig. 3. Hormone metabolism alterations in leaf and fruit of *LCYB*-expressing tomato lines. (A) Phenotype of 18-days old tomato wild type (IPA6+, R.S., and IPA6-) and *LCYB* transgenic lines (pNLyc#2, H.C., and LCe) seedlings grown on MS media. **(B)** Radicle emergence ($n = 8$; three petri dishes). **(C)** Cotyledon opening ($n = 8$; three petri dishes). **(D)** Root length ($n = 5$). **(E)** Biomass ($n = 5$–9). **(F)** Hormone quantification (hormonomics) in leaves and fruits of wild type and transgenic *LCYB* lines. **(G)** GA quantification in leaves and fruits of wild type and transgenic *LCYB* lines by UHPLC-QQQ-MS/MS. Leaf samples were collected from the 5th leaf of six-week-old tomato plants. Fully ripened fruits were collected from 16-week-old tomato plants ($n = 5$; each biological replicate comprising a pool of 3 fruits). Unpaired two-tailed Student t-test was performed to compare transgenic lines with the wild type. In **B–C**, *: $p < 0.05$, **: $p < 0.005$ ***: $p < 0.0005$; in **F**, *: $p < 0.05$. wt: wild type; R.S.: Red Setter; H.C.: high carotene; LCe: lycopene β-cyclase from *Erwinia*; LOD: limit of detection; F.C.: fold change.

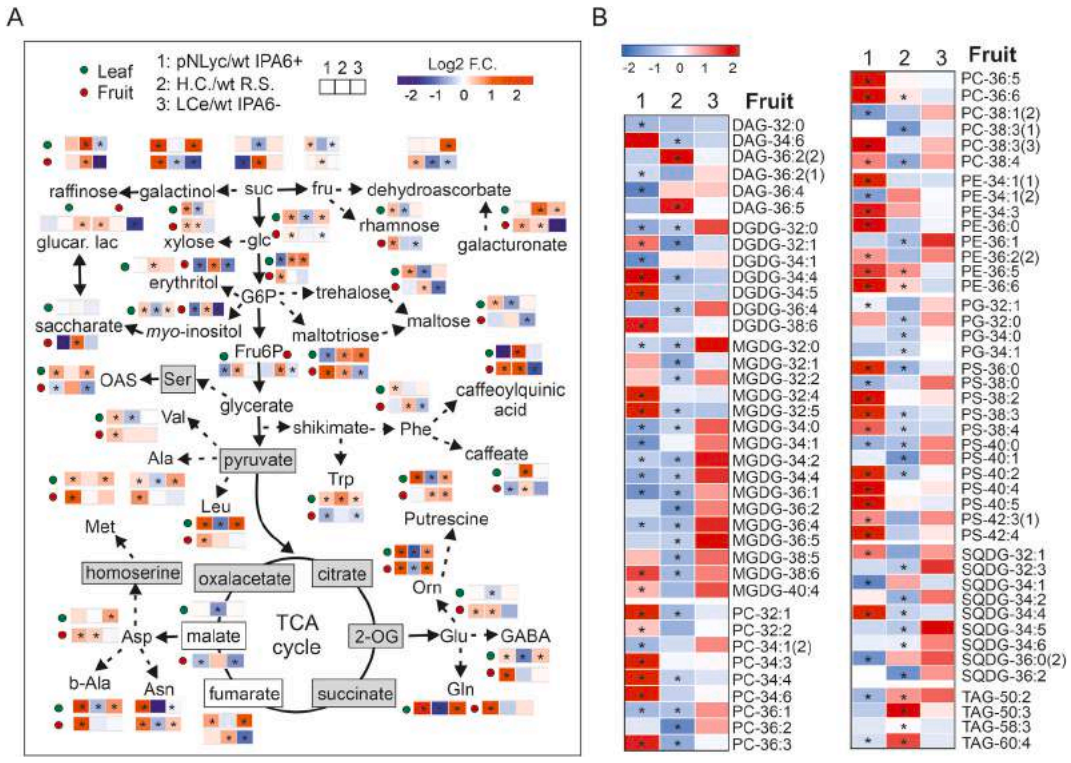

Fig. 4. Metabolic reshaping in leaves and fruits by *LCYB* expression in tomato. (A) Primary metabolite profiling in leaves and fruits (green and red circles, respectively) of wild type (IPA6+, R.S., and IPA6-) and *LCYB* transgenic tomato lines (pNLyc#2, H.C., and LCe). Ratios between pNLyc#2/IPA6+ (1; left), H.C./R.S. (2; middle), and LCe/IPA6 (3; right) lines are shown. A non-paired two-tailed Student t-test was performed to compare each transgenic line with their wild type ($p < 0.05$; $n = 5$). **(B)** Lipid profile in fruits of *LCYB* transgenic tomato lines. The lipid profile in leaves is reported; however, no significant changes were observed (Fig. S16). Wilcoxon's test was performed to compare transgenic lines with their wild types ($p < 0.05$; $n = 5$). Changes are shown as the Log2 fold change between the transgenic lines and their respective wild type controls (for more details see Fig. S15-16). Asterisks represent significant changes. OG: oxoglutarate; orn: ornithine; GABA: gamma aminobutyric acid; suc: sucrose; fru: fructose; glc: glucose; G6P: glucose-6-phosphate; Fru6P: fructose-6-phosphate; OAS: o-acetylserine; glucar. lac: glucarate-1,4-lactone; DAG: diacylglycerol; DGDG: di-galactosyldiacylglycerol; MGDG: mono-galactosyldiacylglycerol; PC: phosphatidylcholine; PE: phosphatidylethanolamine; PG: phosphatidylglycerol; PS: phosphatidylserine; SQDG: sulfoquinovosyl diacylglycerol; TAG: triacylglycerol.

H.C. line (Fig. 3G). In the fruit, however, GA_1 and GA_3 were enhanced in transplastomic pNLyc#2 and LCe lines, while GA_3 and GA_4 were reduced in the H.C. and LCe lines, respectively (Fig. 3G).

3.4. *Primary metabolites and lipid metabolism are altered in leaves and fruits of LCYB-expressing lines*

The strong changes in pigment, hormone, and apocarotenoid contents led us to investigate the impact of these changes on other metabolic pathways. GC-MS metabolite profiling showed significant changes in sucrose and its derivatives (e.g., fructose, galactinol, raffinose), glycolytic intermediates (e.g., glucose, G6P, Fru6P) and TCA cycle intermediates (e.g., malate and fumarate) in the leaves and fruit of the transgenic lines (Fig. 4A; Fig. S16). These changes were reflected, for instance, in changes in G6P-derived compounds (e.g., trehalose, maltotriose, maltose, *myo*-inositol, and erythritol) and amino acids derived from glycerate (e.g., O-acetylserine [OAS]), pyruvate (e.g., valine, alanine, leucine), shikimate (e.g., phenylalanine and tryptophan), malate (e.g., aspartic acid, asparagine, β-alanine, and methionine), and 2-oxoglutarate (e.g., glutamic acid, glutamine, GABA, and ornithine) (Fig. 4A). In addition, due to the structural function of carotenoids (β-carotene and xanthophylls) in membrane composition, together with lipids, we determined the lipid composition in leaves and fruit. Lipid profiling revealed no significant differences in the leaves, while marked significant differences were observed, mainly for structural lipids, in the fruit of pNLyc#2 and H.C. lines (Fig. 4B; Fig. S17). In the fruit of pNLyc#2, a total of 17 galactolipids (GLs) (e.g., mono- and di-galactosyldiacylglycerol, [MGDG and DGDG, respectively]) and 32 phospholipids (PLs) (e.g., phosphatidylcholine [PC], phosphatidylethanolamine [PE], phosphatidylglycerol [PG], and phosphatidylserine [PS]) exhibited significant changes in their abundances (Fig. 4B), with levels of nine GLs being reduced and eight being increased, while the trend for PLs differed, where abundance rations were reduced for seven PLs and increased for 25 PLs. The general trend for sulfolipids (SLs) (e.g., sulfoquinovosyl diacylglycerol [SQDG]) and di- and tri-acylglycerols (DAGs/TAGs) was a reduced abundance, with the exception of two SL species (Fig. 4B). By contrast, in the H.C. line, most of the lipid species that showed significantly different levels displayed a reduced abundance, with a few exceptions (e.g., two DAGs, four TAGs, one PC, and two PEs) that showed increased content (Fig. 4B).

3.5. *Photosynthetic parameters are influenced by carotenoid accumulation and plant architectural changes in tomato LCYB-expressing lines*

The changes in plant growth and architecture induced by modifications in pigment and hormone contents prompted subsequent analysis of several photosynthetic parameters. Photosynthetic measurements were performed in tomato plants (49 days old) grown under greenhouse conditions (Fig. S18). CO_2 assimilation was significantly increased for the H.C. line, relative to its wild type, whereas the transplastomic lines were the same as their wild types (Fig. 5A). Despite some unaltered photosynthetic parameters, the ΦPSII, which reflects plant fitness, was increased in all the lines (Fig. 5A). Interestingly, NPQ(T) was reduced in the H.C. line but was unaltered in the transplastomic lines, in agreement with the observed ΦNPQ (Fig. 5A and Fig. S18H). Conductance was also

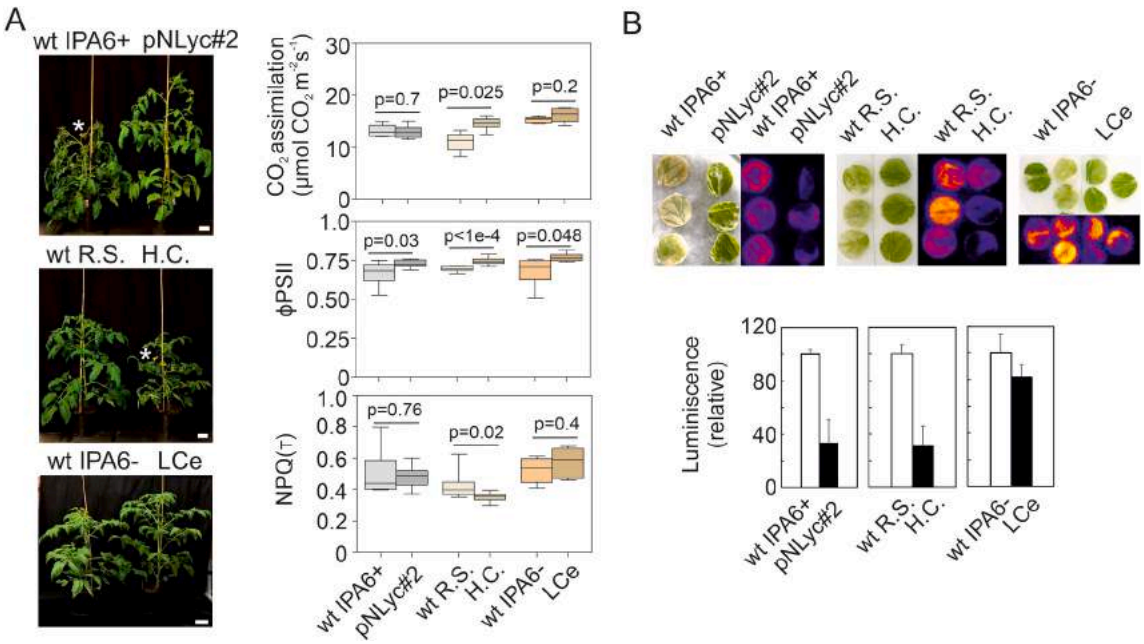

Fig. 5. Photosynthetic parameters and high light tolerance in transgenic *LCYB* tomato lines. (A) Plant phenotypes and CO_2 assimilation, ΦPSII, and total non-photochemical quenching (NPQT) measurements. CO_2 assimilation was measured with a Li-Cor instrument and ΦPSII and NPQT with a MultiSpec instrument (Photosync). Photosynthetic parameters were measured from leaves of seven-week-old wild type (IPA6+, R.S., and IPA6-) and transgenic (pNLyc#2, H.C., and LCe) tomato lines grown under greenhouse conditions. All measurements, and especially NPQT, were performed without a dark adaptation period, as described in Tietz et al. Five to 12 biological replicates (n = 5–12) were used for each photosynthetic measurement. White asterisks in tomato photographs indicate the flowers. **(B)** Lipid peroxidation imaging and quantification of tomato leaf discs (six-week-old plants; n = 3) exposed to a light intensity of 2000 μmol photons m^{-2} s^{-1} and a temperature of 7 °C. A non-paired two-tailed Student t-test was performed to compare transgenic lines with the wild type. wt: wild type; R.S.: Red Setter; H.C.: high carotene; LCe: lycopene β-cyclase from *Erwinia*.

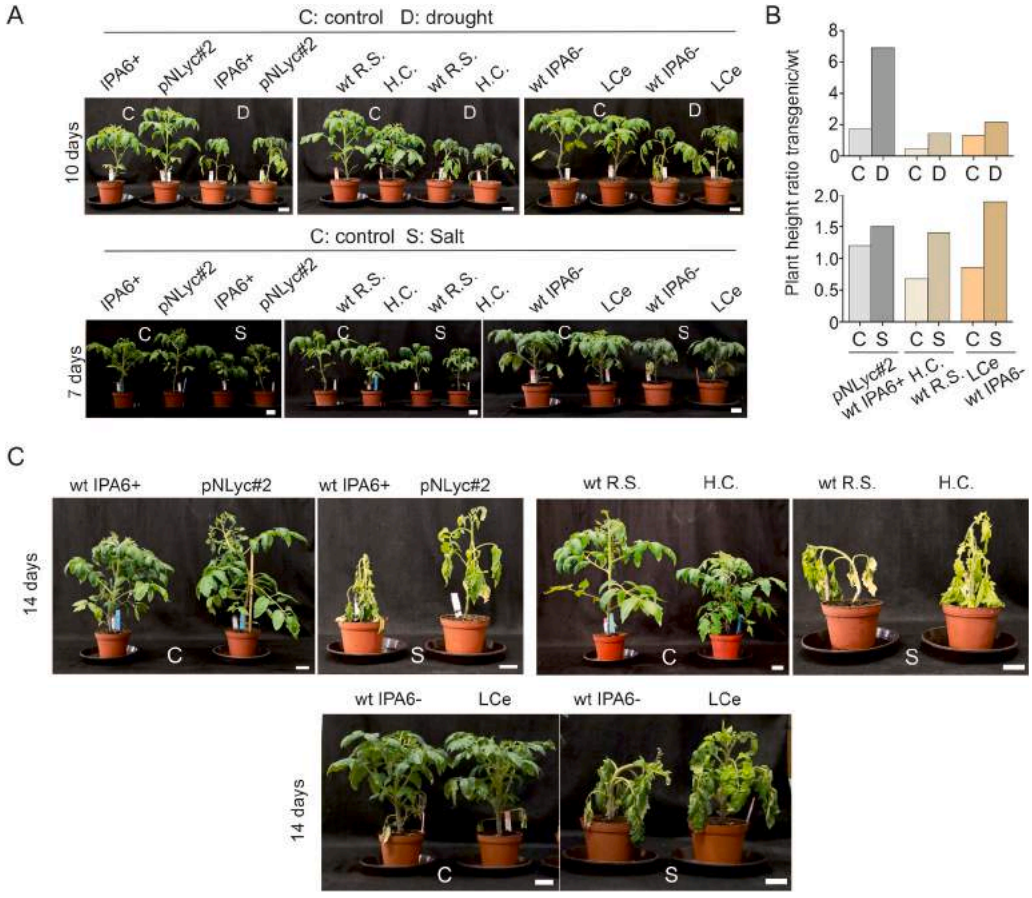

Fig. 6. Abiotic stress tolerance in transgenic LCYB tomatoes. (A) Water deficit and salt treatments in three-week-old wild type and transgenic lines (n = 5–6) grown in the greenhouse (see material and methods). Plant height was recorded before and after water deficit and salt treatments. **(B)** Plant height difference between transgenic lines and their respective wild type controls (plant height ratio). Plant height was measured before (0 days) and after stress onset (10 days for water deficit and seven days for salt treatments) and the plant height rate was calculated under control and under stress conditions. **(C)** Tomato plants subjected to control and salt treatment were recorded after 14 days of stress onset (salt treatment was stopped at day seven). A non-paired two-tailed Student t-test was performed to compare transgenic lines with the wild type. wt: wild type; R.S.: Red Setter; H.C.: high carotene; LCe: lycopene β-cyclase from *Erwinia*. Scale bar: 10 cm.

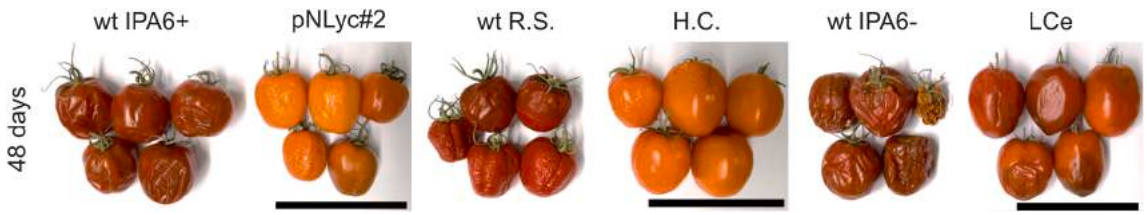

Fig. 7. Tomato fruit shelf life. Tomato fruits from wild type (IPA6+, R.S., and IPA6-) and transgenic lines (pNLyc#2, H.C., and LCe) were harvested ($n = 5$) from three months old tomato plants and stored at room temperature in the laboratory. Tomato fruit comparison between wild type and transgenic lines after 48 days of plant detachment (for full time-point comparison see Fig. S19). wt: wild type; R.S.: Red Setter; H.C.: high carotene; LCe: lycopene β-cyclase from Erwinia. Scale bar: 10 cm.

Table 1
Summary of phenotypic and molecular changes in leaves and fruits of transgenic LCYB-expressing tomato lines.

	Leaf/Shoot			Fruit		
Phenotype	pNLyc#2	H.C.	LCe	pNLyc#2	H.C.	LCe
Plant height	increased	reduced	increased	–	–	–
Leaf number	n.c.	reduced	n.c.	–	–	–
Internode length	increased	reduced	increased	–	–	–
Photosynthesis	n.c.	increased	n.c.	–	–	–
Days to flowering	increased	reduced	n.c.	–	–	–
Fruit number	–	–	–	n.c.	increased	n.c.
Fruit size	–	–	–	n.c.	increased	increased
Stem D.W.	increased	reduced	n.c.	–	–	–
Leaf D.W.	n.c.	n.c.	increased	–	–	–
Fruit D.W.	–	–	–	n.c.	increased	n.c.
β-carotene	n.c.	reduced	reduced	increased	increased	increased
Xanthophylls	increased	increased	reduced	reduced	reduced	n.d.
β-cyclocitral	reduced	reduced	reduced	increased	increased	reduced
Zaxinone	reduced	reduced	n.c.	n.c.	reduced	increased
ABA	increased	reduced	reduced	increased	increased	n.c.
SA	n.c.	n.c.	n.c.	increased	n.c.	n.c.
iP	n.c.	n.c.	n.c.	increased	reduced	increased
GA_1	n.c.	increased	reduced	< LOD	< LOD	< LOD
GA_4	< LOD	< LOD	< LOD	< LOD	< LOD	< LOD
IAA	n.c.	increased	n.c.	reduced	reduced	increased
JA	increased	n.c.	increased	increased	increased	n.c.
JA-Ile	< LOD	< LOD	increased	increased	increased	n.c.
H.L. tolerance	increased	increased	n.c.	–	–	–
Drought tolerance	increased	increased	increased	–	–	–
Salt tolerance	increased	increased	increased	–	–	–
Shelf life	–	–	–	increased	increased	increased

*<LOD: below limit of detection; n.c.: not changed; R.S.: Red Setter; H.C.: high carotene; LCe: lycopene β-cyclase from *Erwinia*.

reduced in the pNLyc#2 line and increased in the H.C. and LCe lines (Fig. S18F). The rETR was unchanged in the pNLyc#2 and LCe lines but was increased in the H.C. line (Fig. S18G). These results suggest that the nuclear H.C. line is the one with the most enhanced photosynthetic efficiency, despite its smaller shoot size.

3.6. LCYB-expressing lines show enhanced abiotic stress tolerance and shelf life

The increases in xanthophyll and hormone contents were further assessed, given their functions in photoprotection and stress tolerance, by exposing the transgenic lines to several abiotic stresses. Leaves of the pNLyc#2 and H.C. transgenic lines, which had higher xanthophyll content, showed enhanced high light tolerance compared to the wild type, as measured by the luminescence produced by the accumulation of lipid peroxides (Fig. 5B). The LCe line showed no significant increase in high light tolerance (Fig. 5B). In addition, tomato plants were exposed to water deficit by stopping irrigation for 10 days. In order to analyze the impact of water deficit on plant growth we used plant height as a growth parameter and measured it before (0 days) and after (10 days) stress application for control (watered plants) and stressed plants (Fig. S19A). Based on that data we calculated a plant height ratio between the transgenic line and its wild type under control and stress conditions to determine which lines were better adapted to the stress conditions. Interestingly, plant height ratios obtained under water deficit were higher than the plant height ratios obtained under control conditions (pNLyc#2/390%, H.C./297%, and LCe/40%) suggesting that the transgenic lines are better adapted to the water deficit conditions (Fig. 6A–B). We used the same rationale to assess salt tolerance in the tomato lines. However, we watered the control plants only with water while treated plants were watered with a NaCl (200 mM) solution for seven days (Fig. S19B). With the obtained plant height measurements (Fig. S19B) we calculated the plant height ratios for the transgenic and wild type lines. In this case, transgenic lines also grew much better (pNLyc#2/27%, H.C./205%, and LCe/210%) than the wild type under stress conditions compared to their plant height ratio calculated under control conditions (Fig. 6A–B). This became more evident after one week of recovery phase after seven days of salt treatment where the wild type lines were severely affected when compared with their transgenic lines (Fig. 6C).

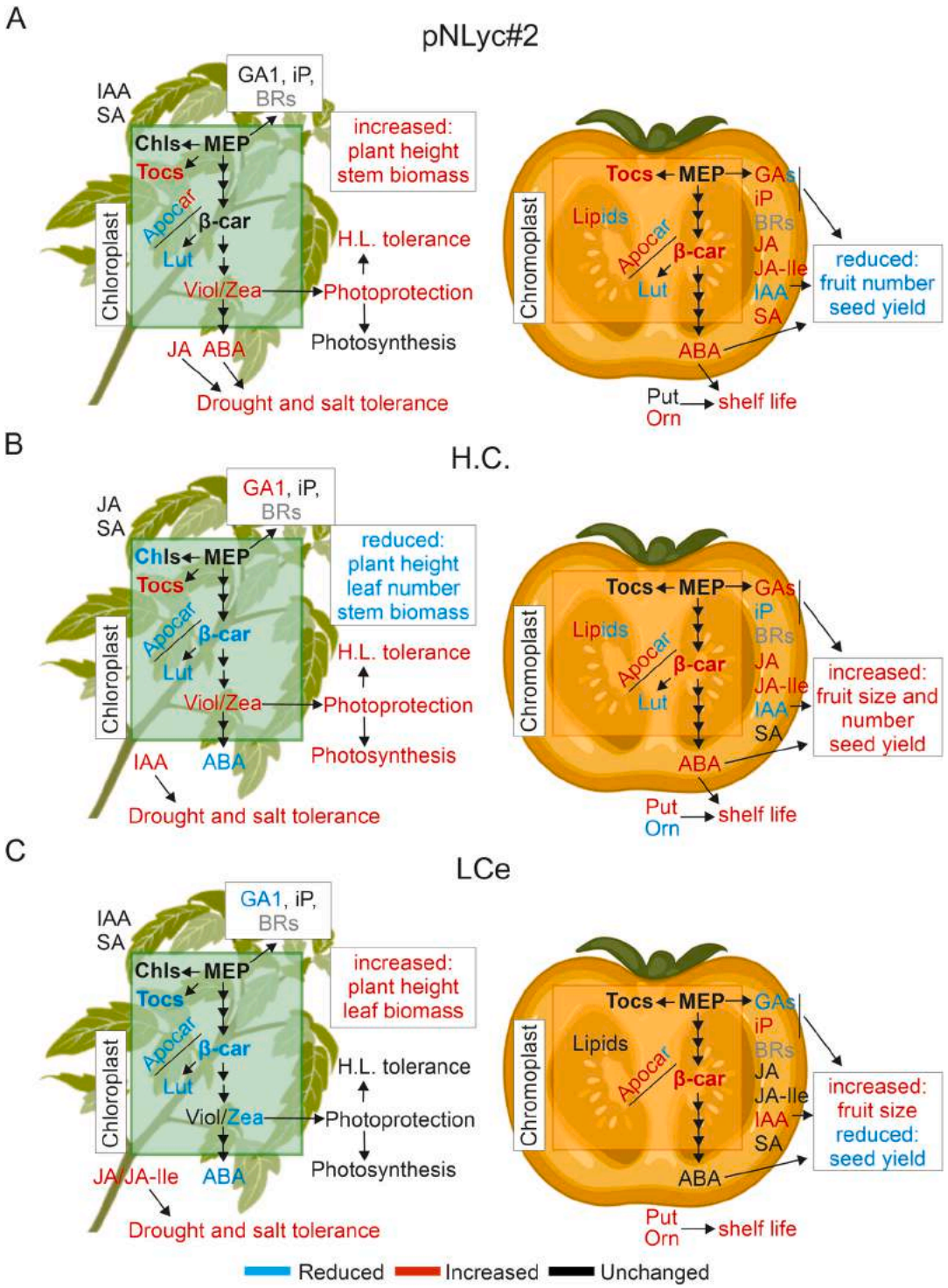

Fig. 8. Schematic representation of physiological and metabolic changes in *LCYB* transgenic tomatoes. Physiological and metabolic changes in leaf (leaf) and fruits (right) in pNLyc#2 **(A)**, H.C. **(B)**, and LCe **(C)** transgenic tomato lines. Increases (red), reductions (blue), no changes (black), or compounds under the limit of detection by the hormonomics approach (grey), are shown. Put: putrescine; Orn: ornithine; Lut: lutein; β-car: β-carotene; Tocs: tocopherols; Chls: chlorophylls; Apocar: apocarotenoids; GAs: gibberellins; Viol: violaxanthin; Zea: zeaxanthin; BRs: brassinosteroids; iP: isopentenyladenine. The figure was prepared using Biorender.com.

An extended fruit shelf-life has previously been reported in tomato and other fruits due to enhanced ABA content (Diretto et al., 2020) or to the content of other primary metabolites (e.g., putrescine), so we also examined fruit shelf-life in the transgenic lines. All transgenic lines showed enhanced shelf-life at different time points after harvest when compared to their respective wild types (Fig. 7 and Fig. S20).

4. Discussion

The tomato is one of the most important food crops worldwide, but its productivity is affected by several abiotic stresses that have deleterious effects on fruit size, quantity, and quality (Gerszberg and Hnatuszko-Konka, 2017). Here, we showed that the introduction of

different *LCYB* genes influences tomato plant fitness, stress tolerance, and biomass, regardless of its genetic origin, tomato cultivar, or genetic transformation strategy (Table S1). However, the use of different cultivar backgrounds, transformation methods, and transgene source, contributed to particular differences observed in the plant phenotypes. In fact, plastid DNA from pNLyc#2 and LCe lines was transformed with particle bombardment using the vectors pNLyc (Apel and Bock, 2009) and pRB96 (Wurbs et al., 2007), respectively. The pNLyc vector contains the strong ribosomal RNA operon promoter (*Prrn*) fused to the 5′ leader of the gene 10 of phage T7 (Kuroda and Maliga, 2001), which enhances the transcription of the daffodil *LCYB* gene. The pRB96 vector contains the promoter of the plastid *atpI*, which contains multiple binding sites for the RNA polymerases present in higher plant plastids (Wurbs et al., 2007), driving the expression of the Erwinia *LCYB* gene. Moreover, plastid transformation vectors are based on homologous recombination which allow the insertion of the transgenes in a single copy and in the same position of the plastid genome, avoiding the positional effect introduced by agrobacterium-mediated plant transformation. In addition, agrobacterium-mediated plant transformation can introduce a transgene in single, double and sometimes even multiple copies affecting directly the expression level of the transgene. The H.C. line was transformed with the pJLcy vector (D'Ambrosio et al., 2004) via agrobacterium-mediated transformation. The pJLcy vector contains the cauliflower mosaic virus 35S promoter and directs the expression of the tomato *LCYB* gene. Besides the clear differences between the transformation methods, promoters, and transgenes, the different cultivar background add another layer of complexity to our comparison. Although all three cultivars are processing and high yield varieties, IPA6+ contains lutein while IPA6-don't (Wurbs et al., 2007). Differences in carotenoid content in the different cultivars could indirectly impact the accumulation of apocarotenoids or phytohormones. Considering the above-mentioned differences, the results discussed below may vary in transgenic lines with different cultivar background, genetic transformation method and transgene source.

The lycopene β-cyclase (LCYB) catalyzes the conversion of lycopene to β-carotene, a step previously characterized as a metabolic hot spot in tobacco (Kossler et al., 2021; Moreno et al., 2020). The metabolic hot spot focused on β-carotene reflects its multiple functions in several molecular and physiological processes (e.g., photosynthesis, oxidative stress). β-Carotene serve as precursor of xanthophylls (photoprotection), hormones (growth/development/stress response), and growth regulators. Thus, changes in carotenoid content could directly influence photosynthesis, antioxidant properties, and pigment content, while indirectly influencing hormone and apocarotenoid content (ABA, SLs, β-cc) and, consequently, plant growth and stress responses (Al-Babili and Bouwmeester, 2015; Nambara and Marion-Poll, 2005; Wang et al., 2019).

In fact, the transgenic tomato lines analyzed here are evidence of carotenoids as a metabolic hot spot because, despite the differences in their genetic background, these tomato lines universally displayed changes in carotenoids, apocarotenoids, and hormone contents (Figs. 2–3) that resulted in altered growth regulation and biomass partitioning in different tissues and under different climate conditions (Fig. 1 and Figs. S1-4). The hormonal changes and their effects on primary metabolism can explain the changes in biomass accumulation and stress tolerance (Moreno et al., 2020, 2021a; Sheyhakinia et al., 2020; Yoshida et al., 2014). For instance, gibberellins (GAs) control many aspects of growth and plant development. Bioactive GAs (GA_4, GA_3, GA_1) function as key players in plant growth (longer stems and leaf internodes) and development in Arabidopsis, tobacco, and rice, with GA_4 showing the highest bioactivity (Cowling et al., 1998; Gallego-Giraldo et al., 2008; Talon et al., 1990; Ueguchi-Tanaka et al., 2007). Moreover, exogenous application of GAs (GA_4, GA_3, GA_1) to MS media resulted in plants with longer stems and internodes, while GA inhibitor application resulted in the opposite effect (Kossler et al., 2021; Moreno et al., 2020). Higher accumulation of GA_4 and GA_1 in pNLyc#2 and LCe transplastomic lines, respectively, is in line with their longer stems and leaf internodes, while shorter stem and leaf internodes in H.C. tomatoes reflect their lower GA_3 accumulation (Fig. 1A–C, J and Fig. 3G; Fig. S18A, D). This reduced-growth phenotype might be also related with the reduced plant size previously reported in ABA-deficient mutants of tomato (Nitsch et al., 2012). However, a similar ABA reduction in LCe (longer stem and internodes), suggests that the interaction between GAs and ABA might direct plant height, as previously observed in *DcLCYB1* tobacco plants (Moreno et al., 2020). In addition, reductions in β-cyclocitral and/or zaxinone in the transplastomic lines (Fig. 2B) suggest that they do not influence the observed growth phenotype, while reductions in both metabolites might contribute to the smaller growth phenotype observed in the H.C. line (Fig. 1B).

In terms of abiotic stress tolerance, ABA is one of the most important plant hormones conferring salt and drought stress tolerance, however, ABA-independent pathways resulting in salt and/or drought tolerance have been reported (Yoshida et al., 2014). For instance, enhanced JA/JA-Ile and IAA contents conferred salt and drought tolerance in Arabidopsis, white clover, and rice (Hazman et al., 2019; Kazan, 2015; Shani et al., 2017; Sharma et al., 2013; Shi et al., 2014; Zhang et al., 2020). The enhanced ABA and JA ($p = 1.1e^{-3}$ and $p = 4e^{-3}$; Fig. 3F and Fig. S9) contents in pNLyc#2 transgenic line might contribute to its enhanced salt and drought tolerance (Fig. 6 and Fig. S19), as previously shown in Arabidopsis and tobacco (Kazan, 2015; Moreno et al., 2020, 2021a; Yoshida et al., 2014). In addition, the enhanced ABA content may have caused stomatal closure, as reflected in the observed reduction in stomatal conductance (Fig. S18F). This reduction would conceivably impede an enhancement of photosynthetic efficiency (Fig. 5A–B, and Fig. S18F-I). By contrast, the H.C. and LCe lines displayed a slightly reduced ABA content and enhanced stomatal conductance; however, only the H.C. line showed enhanced photosynthetic efficiency (higher CO_2 assimilation, rETR, and ΦPSII; Fig. 5A–B, and Fig. S18F-I). Although these lines showed reduced ABA content, they both showed enhanced salt and drought tolerance, suggesting the participation of an ABA-independent pathway. In fact, JA/JA-Ile are involved in salt and drought tolerance in Arabidopsis and rice (Hazman et al., 2019; Kazan, 2015). The increases in JA and JA-Ile contents ($p = 0.05$ and $p < 1e^{-4}$; Fig. 3F and Fig. S9) in the LCe line is in line with the higher drought and salt tolerance observed in this line. However, the H.C. line showed a reduction in ABA and no changes in JA, but a significant increase in IAA ($p = 0.03$; Fig. 3F and Fig. S9). IAA has been reported to enhance salt and drought tolerance in white clover, Arabidopsis, and rice (Shani et al., 2017; Sharma et al., 2013; Shi et al., 2014; Zhang et al., 2020), and thus, most likely also in the H.C. transgenic line (Fig. 6 and Fig. S19). Nevertheless, several osmoprotectants, which help organisms to cope with severe osmotic stress (Singh et al., 2015), were enhanced in the transgenic lines (Fig. 4A). Increased ABA and JA contents were previously reported to enhance the synthesis of osmoprotectants (e.g., sugars, polyamines) under abiotic stress conditions to counteract harmful effects (Alcazar et al., 2006; Sheyhakinia et al., 2020; Toumi et al., 2010; Wang et al., 2020). In line with this evidence, increases in sugars (i.e. glucose, trehalose), sugar alcohols (i.e. *myo*-inositol) and polyamines (putrescine) in leaves can also contribute to enhanced abiotic stress tolerance in our transgenic lines (Figs. 4A and 6 and Fig. S19; Table S4).

Although some common and specific hormonal changes were quantified in the transgenic lines, the precise mechanism explaining different hormone accumulation in each transgenic line remained elusive. One possible explanation of the different hormone alterations in the transgenic lines (besides cultivar background, transformation method, and origin of the transgene) might be the impact of the *LCYB* gene expression on other isoprenoid pathways. Feedback mechanisms between carotenoids, methylerythritol phosphate (MEP), and ABA pathways, can also influence carotenoid accumulation in maize, rice, Arabidopsis, and tomato (Bai et al., 2009; Beyer et al., 2002; Qin et al., 2007; Romer et al., 2000). For instance, enhanced *PSY* expression in etiolated Arabidopsis seedlings also resulted in enhanced carotenoid

levels via post-translational accumulation of *DXS* mRNA, which stimulated the supply of MEP substrates (Rodriguez-Villalon et al., 2009a, 2009b). Thus, any alteration in the expression of a carotenogenic gene can impact the expression of other carotenoid genes, as well as key genes (but also metabolite/hormone content such as chlorophylls and GA) from other isoprenoid pathways (e.g., MEP, GAs), as previously observed in *DcLCYB1* tobacco lines (Moreno et al., 2020). In fact, our tomato lines also showed altered levels of chlorophylls and tocopherols in both leaf and fruit (Fig. S6). Notably, isoprenoids are also the precursors of GAs, brassinosteroids, and CKs, so any disturbance in the isoprenoid flux might influence isoprenoid-derived hormone contents, with subsequent impacts on plant growth, development, or stress tolerance (Gudesblat and Russinova, 2011; Ha et al., 2012; Hedden and Phillips, 2000; Krishna, 2003; Schaller et al., 2015; Tran et al., 2007).

The increased xanthophyll content in leaves could further enhance photoprotection and therefore impart high light tolerance (pNLyc#2 and H.C.; Fig. 5B). In the fruit, stronger increases in β-carotene content caused stronger changes in hormone content, thereby impacting fruit and seed productivity (Figs. 1–2, Fig. 3F–G, and Figs. S2 and S5; Table S5), making the fruit rich in pro-vitamin A and enhancing its nutritional value. Fruit growth is influenced by CKs, Aux, GA, and ABA (Quinet et al., 2019). GA_1, was reported to be one of the most bioactive GA influencing fruit growth (Garcia-Hurtado et al., 2012). However, in the case of pNLyc#2 line, the enhanced GA_1 and GA_3 does not trigger enhanced fruit growth/biomass while the LCe line with similar increases and a reduction in GA_4 content showed enhanced fruit growth//biomass (Fig. 1 and Fig. S2J). The reduction in GA3 in the line H.C. did not correlate with the highest increase in size and biomass observed in this line and thus suggest that GA might not be the only components determining fruit size and growth but also the content of other hormones such as CKs, Aux, and ABA (Quinet et al., 2019). Furthermore, changes in the hormonal network might confer additional advantages to the fruit. Recently, Diretto et al. showed that the enhanced shelf-life of *LCYB*-expressing tomato lines was due to increased ABA content and its negative impact on ethylene content (Diretto et al., 2020). Increased ABA content in the pNLyc#2 and H.C. lines conferred longer fruit shelf-life compared to the wild type (Fig. 7 and Fig. S20). However, in the LCe line, which also showed enhanced shelf-life, the ABA content was unchanged, suggesting that shelf-life might be controlled by other factors. Indeed, polyamines (e.g., spermidine, putrescine) are known anti-senescence agents which increase fruit firmness, delay ethylene emission and the climacteric respiratory burst, and induce mechanical stress resistance (Valero et al., 2002). The highest ornithine and putrescine content ($p < 0.05$) was observed in the LCe line, and this could contribute to its enhanced shelf-life (Figs. 4A and 7; Table S5). Accumulation of sugars and derivatives (e.g., raffinose, galactinol, *myo*-inositol, and trehalose) and amino acids (e.g., Val, Asp, Asn, Thr, Glu, Gln, and Ala) in fruit were reported to confer tolerance to chilling injury and resistance to pathogens and several postharvest stress conditions (Bang et al., 2019; Farcuh et al., 2018; Lauxmann et al., 2014; Luengwilai et al., 2018). Accumulation of these metabolites would be expected to confer valuable post-harvest traits to our tomatoes apart from the enhanced shelf-life and their higher pro-vitamin A content.

Interestingly, several apocarotenoids were reported to have a key role in biotic interactions (e.g., β-ionone, loliolide, mycorradicin, blumenols) (Caceres et al., 2016; Moreno et al., 2021b). For instance, β-ionone and loliolide were reported to play key roles in plant defense to herbivores (Caceres et al., 2016; Murata et al., 2019) while mycorradicin and blumenols are important for arbuscular mycorrhiza (AM) establishment and functioning (Moreno et al., 2021b). Since β-carotene and zeaxanthin are the precursor of these apocarotenoids, and leaves and fruits of our transgenic tomato lines showed enhanced β-carotene content it might not be surprising if biotic interactions in different tissues could be influenced. In fact, our tomato fruits showed enhanced β-ionone content (pNLyc#2 and H.C.; Fig. S11) which might suggest enhanced plant defense against herbivores. Unfortunately, we did not evaluate carotenoid and apocarotenoid metabolism in roots, but it is likely that their metabolism it is also affected, and thus, we cannot rule out an impact in AM establishment. To confirm these possibilities pathogen and mycorrhization experiments must be done with these lines. The possible increment in apocarotenoids and phytohormones influencing biotic interactions by the enhancement of carotenoids will be a great tray especially for cereal crops such as rice, wheat, and/or barley since they do not accumulate carotenoids (or at very low amount). By doing so, cereal crops will have enhanced provitaminA content, and they could positively benefit from enhanced biotic interactions.

The use of transgenic tomato lines with different cultivar and genetic backgrounds allowed us to demonstrate that i) *LCYB* overexpression can be used to modulate growth (biomass partitioning between leaf and fruit) and fruit yield in a crop, and ii) the positive growth regulatory effect conferred by the carrot *DcLCYB1* gene in tobacco (Moreno et al., 2020) can be also conferred by other LCYBs (e.g., tomato, daffodil, and bacteria) in leaves and/or fruit. However, the different genetic origins of the chosen *LCYB* genes also introduced specific changes in each line (Table 1; Fig. 8). Therefore, a seemingly simple introduction of a single transgene might result in unpredictable changes at molecular, metabolic, and phenotypic level.

In conclusion, while some of the differences at the phenotypic and metabolic levels observed in the transgenic lines might reside in the different cultivars, transformation methods, and *LCYB* genetic origins, many similarities can be explained by the modulation of molecular processes, such as carotenoid and hormone accumulations (Table 1; Fig. 8). Despite the observed specific changes in carotenoid, hormone, and metabolite accumulation in leaves and fruit of the transgenic lines (Table 1, S4-5; Fig. 8), the similar responses in these lines can be attributed to changes in specific hormones (salt and drought tolerance are most likely conferred by increases in ABA and JA for pNLyc#2, IAA for H.C., and JA and JA-Ile for LCe) and/or metabolites (e.g., ABA- and/or putrescine-enhanced shelf-life). However, other contrasting phenotypes were probably caused by specific interactions between hormones and/or their ratios, as well as the connection between carotenoids and other non-isoprenoid hormones (IAA), which remain to be investigated. Nevertheless, modulation of the content of main components of the hormonal network in each transgenic line resulted in enhanced abiotic stress tolerance, extended fruit shelf life, and increased biomass (favoring shoot and/or fruit in the different lines), along with the enhanced nutritional value conferred by the higher β-carotene content in the fruit. All these features are highly desirable traits for crop improvement (enhanced stress tolerance and biomass/yield) considering the worldwide climate change and its consequences for food crop production. This type of bioengineering is a promising strategy that can be exported to cereal crops (e.g., rice) that, in general, do not accumulate high levels of carotenoids but whose yield must be greatly increased by 2050.

Author contributions

J.C.M: Conceived the project and the experimental design, performed growth, biomass and yield, salt and drought stress, and fruit shelf-life experiments. J.G.V. and J.C.M.: performed photosynthetic experiments with Li-Cor and Multispec, respectively, and performed metabolite extraction and sample preparation (J.C.M.), and data analysis (J.G.V.). J.M. and S.A.: performed apocarotenoid and gibberellins extraction, sample preparation and data analysis. O.N. and I.P.: performed hormonomics analysis. M.R–C.: performed carotenoid extraction and quantification; S.C. and J.C.M.: performed data analysis from lipidomics and lipid extraction, respectively. M.H.: performed high light stress experiments and lipid peroxide quantification. M.K. and J.C.M.: performed microscopy analysis with assistance of J.C.M. JCM wrote the paper with special input from A.R.F., M.R–C., A.S. and all other coauthors.

Data availability

All data is provided within the main body or the supplemental information (SI) and data sets (SD).

Declaration of competing interest

The authors declare no conflict of interest.

Acknowledgments

We are grateful to Prof. Dr. Lothar Willmitzer for his support and advice. We thank Prof. Dr. Ralph Bock (Max Planck Institute of Molecular Plant physiology, Golm, Germany) and Dr. Caterina D'Ambrosio (Centro Ricerche Metapontum Agrobios, ALSIA, Italy) for kindly providing the transplastomic pNLyc#2 and LCe seeds and the homozygous nuclear High Caro (H.C.) lines, respectively. We thank Dr. Camila Caldana and Anne Michaelis for providing the GC facility and running the GC samples, respectively, and Maria Rosa Rodriguez-Goberna for technical support related with pigment analysis (supported by grant BIO2017-84041-P from the Spanish AEI). In addition, we thank Hana Martínková and Petra Amakorová for their help with phytohormone analyses. The hormonomics work was funded by the Ministry of Education, Youth and Sports of the Czech Republic (European Regional Development Fund-Project "Plants as a tool for sustainable global development" No. CZ.02.1.01/0.0/0.0/16_019/0000827), and the Internal Grant Agency of Palacký University (IGA_PrF_2021_011).

Appendix A. Supplementary data

Supplementary data related to this article can be found at https://doi.org/10.1016/j.ymben.2022.01.004.

References

Al-Babili, S., Bouwmeester, H.J., 2015. Strigolactones, a novel carotenoid-derived plant hormone. Annu. Rev. Plant Biol. 66, 161–186.
Alcazar, R., Cuevas, J.C., Patron, M., Altabella, T., Tiburcio, A.F., 2006. Abscisic acid modulates polyamine metabolism under water stress in Arabidopsis thaliana. Physiol. Plantarum 128, 448–455.
Apel, W., Bock, R., 2009. Enhancement of carotenoid biosynthesis in transplastomic tomatoes by induced lycopene-to-provitamin A conversion. Plant Physiol. 151, 59–66.
Bai, L., Kim, E.H., DellaPenna, D., Brutnell, T.P., 2009. Novel lycopene epsilon cyclase activities in maize revealed through perturbation of carotenoid biosynthesis. Plant J. 59, 588–599.
Bang, J., Lim, S., Yi, G., Lee, J.G., Lee, E.J., 2019. Integrated transcriptomic-metabolomic analysis reveals cellular responses of harvested strawberry fruit subjected to short-term exposure to high levels of carbon dioxide. Postharvest Biol. Technol. 148, 120–131.
Beyer, P., Al-Babili, S., Ye, X., Lucca, P., Schaub, P., Welsch, R., Potrykus, I., 2002. Golden Rice: introducing the beta-carotene biosynthesis pathway into rice endosperm by genetic engineering to defeat vitamin A deficiency. J. Nutr. 132, 506S–510S.
Birtic, S., Ksas, B., Genty, B., Mueller, M.J., Triantaphylides, C., Havaux, M., 2011. Using spontaneous photon emission to image lipid oxidation patterns in plant tissues. Plant J. 67, 1103–1115.
Caceres, L.A., Lakshminarayan, S., Yeung, K.K., McGarvey, B.D., Hannoufa, A., Sumarah, M.W., Benitez, X., Scott, I.M., 2016. Repellent and attractive effects of alpha-, beta-, and dihydro-beta- ionone to generalist and specialist herbivores. J. Chem. Ecol. 42, 107–117.
Chong, J., Wishart, D.S., Xia, J., 2019. Using MetaboAnalyst 4.0 for comprehensive and integrative metabolomics data analysis. Curr. Protoc. Bioinformatics 68, e86.
Cowling, R.J., Kamiya, Y., Seto, H., Harberd, N.P., 1998. Gibberellin dose-response regulation of GA4 gene transcript levels in Arabidopsis. Plant Physiol. 117, 1195–1203.
D'Alessandro, S., Ksas, B., Havaux, M., 2018. Decoding beta-cyclocitral-mediated retrograde signaling reveals the role of a detoxification response in plant tolerance to photooxidative stress. Plant Cell 30, 2495–2511.
D'Alessandro, S., Mizokami, Y., Legeret, B., Havaux, M., 2019. The apocarotenoid beta-cyclocitric acid elicits drought tolerance in plants. iScience 19, 461–473.
D'Ambrosio, C., Giorio, G., Marino, I., Merendino, A., Petrozza, A., Salfi, L., Stigliani, A. L., Cellini, F., 2004. Virtually complete conversion of lycopene into beta-carotene in fruits of tomato plants transformed with the tomato lycopene beta-cyclase (tlcy-b) cDNA. Plant Sci. 166, 207–214.
D'Andrea, L., Amenos, M., Rodriguez-Concepcion, M., 2014. Confocal laser scanning microscopy detection of chlorophylls and carotenoids in chloroplasts and chromoplasts of tomato fruit. Methods Mol. Biol. 1153, 227–232.
Dickinson, A.J., Lehner, K., Mi, J., Jia, K.P., Mijar, M., Dinneny, J., Al-Babili, S., Benfey, P.N., 2019. beta-Cyclocitral is a conserved root growth regulator. Proc. Natl. Acad. Sci. U. S. A. 116, 10563–10567.
Ding, F., Wang, M., Zhang, S., Ai, X., 2016. Changes in SBPase activity influence photosynthetic capacity, growth, and tolerance to chilling stress in transgenic tomato plants. Sci. Rep. 6, 32741.
Diretto, G., Frusciante, S., Fabbri, C., Schauer, N., Busta, L., Wang, Z.H., Matas, A.J., Fiore, A., Rose, J.K.C., Fernie, A.R., Jetter, R., Mattei, B., Giovannoni, J., Giuliano, G., 2020. Manipulation of beta-carotene levels in tomato fruits results in increased ABA content and extended shelf life. Plant Biotechnol. J. 18, 1185–1199.
Emiliani, J., D'Andrea, L., Ferreyra, M.L.F., Maulion, E., Rodriguez, E., Rodriguez-Concepcion, M., Casati, P., 2018. A role for beta,beta-xanthophylls in Arabidopsis UV-B photoprotection. J. Exp. Bot. 69, 4921–4933.
Farcuh, M., Rivero, R.M., Sadka, A., Blumwald, E., 2018. Ethylene regulation of sugar metabolism in climacteric and non-climacteric plums. Postharvest Biol. Technol. 139, 20–30.
Fernie, A.R., Aharoni, A., Willmitzer, L., Stitt, M., Tohge, T., Kopka, J., Carroll, A.J., Saito, K., Fraser, P.D., DeLuca, V., 2011. Recommendations for reporting metabolite data. Plant Cell 23, 2477–2482.
Gallego-Giraldo, L., Ubeda-Tomas, S., Gisbert, C., Garcia-Martinez, J.L., Moritz, T., Lopez-Diaz, I., 2008. Gibberellin homeostasis in tobacco is regulated by gibberellin metabolism genes with different gibberellin sensitivity. Plant Cell Physiol. 49, 679–690.
Garcia-Hurtado, N., Carrera, E., Ruiz-Rivero, O., Lopez-Gresa, M.P., Hedden, P., Gong, F., Garcia-Martinez, J.L., 2012. The characterization of transgenic tomato overexpressing gibberellin 20-oxidase reveals induction of parthenocarpic fruit growth, higher yield, and alteration of the gibberellin biosynthetic pathway. J. Exp. Bot. 63, 5803–5813.
Garcia-Molina, A., Leister, D., 2020. Accelerated relaxation of photoprotection impairs biomass accumulation in Arabidopsis. Native Plants 6, 9–12.
Gerszberg, A., Hnatuszko-Konka, K., 2017. Tomato tolerance to abiotic stress: a review of most often engineered target sequences. Plant Growth Regul. 83, 175–198.
Giorio, G., Stigliani, A.L., D'Ambrosio, C., 2007. Agronomic performance and transcriptional analysis of carotenoid biosynthesis in fruits of transgenic HighCaro and control tomato lines under field conditions. Transgenic Res. 16, 15–28.
Gudesblat, G.E., Russinova, E., 2011. Plants grow on brassinosteroids. Curr. Opin. Plant Biol. 14, 530–537.
Ha, S., Vankova, R., Yamaguchi-Shinozaki, K., Shinozaki, K., Tran, L.S., 2012. Cytokinins: metabolism and function in plant adaptation to environmental stresses. Trends Plant Sci. 17, 172–179.
Hazman, M., Suhnel, M., Schafer, S., Zumsteg, J., Lesot, A., Beltran, F., Marquis, V., Herrgott, L., Miesch, L., Riemann, M., Heitz, T., 2019. Characterization of jasmonoyl-isoleucine (JA-Ile) hormonal catabolic pathways in rice upon wounding and salt stress. Rice 12, 45.
Hedden, P., Phillips, A.L., 2000. Gibberellin metabolism: new insights revealed by the genes. Trends Plant Sci. 5, 523–530.
Hou, X., Rivers, J., Leon, P., McQuinn, R.P., Pogson, B.J., 2016. Synthesis and function of apocarotenoid signals in plants. Trends Plant Sci. 21, 792–803.
Hussain, H.A., Men, S., Hussain, S., Chen, Y., Ali, S., Zhang, S., Zhang, K., Li, Y., Xu, Q., Liao, C., Wang, L., 2019. Interactive effects of drought and heat stresses on morpho-physiological attributes, yield, nutrient uptake and oxidative status in maize hybrids. Sci. Rep. 9, 3890.
Kazan, K., 2015. Diverse roles of jasmonates and ethylene in abiotic stress tolerance. Trends Plant Sci. 20, 219–229.
Kopka, J., Schauer, N., Krueger, S., Birkemeyer, C., Usadel, B., Bergmuller, E., Dormann, P., Weckwerth, W., Gibon, Y., Stitt, M., Willmitzer, L., Fernie, A.R., Steinhauser, D., 2005. GMD@CSB.DB: the Golm Metabolome database. Bioinformatics 21, 1635–1638.
Kossler, S., Armarego-Marriott, T., Tarkowska, D., Tureckova, V., Agrawal, S., Mi, J., Perez da Sousa, L., Aurel Schottler, M., Schadach, A., Frohlich, A., Bock, R., Al-Babili, S., Ruf, S., Sampathkumar, A., Moreno, J.C., 2021. Lycopene β-cyclase expression influences plant physiology, development, and metabolism in tobacco plants. J. Exp. Bot. 72 (7), 2544–2569. https://doi.org/10.1093/jxb/erab029.
Krall, J.P., Edwards, G.E., 1992. Relationship between photosystem-ii activity and Co2 fixation in leaves. Physiol. Plantarum 86, 180–187.
Krishna, P., 2003. Brassinosteroid-mediated stress responses. J. Plant Growth Regul. 22, 289–297.
Kromdijk, J., Glowacka, K., Leonelli, L., Gabilly, S.T., Iwai, M., Niyogi, K.K., Long, S.P., 2016. Improving photosynthesis and crop productivity by accelerating recovery from photoprotection. Science 354, 857–861.
Kuhlgert, S., Austic, G., Zegarac, R., Osei-Bonsu, I., Hoh, D., Chilvers, M.I., Roth, M.G., Bi, K., TerAvest, D., Weebadde, P., Kramer, D.M., 2016. MultispeQ Beta: a tool for large-scale plant phenotyping connected to the open PhotosynQ network. R. Soc. Open Sci. 3, 160592.
Kuroda, H., Maliga, P., 2001. Complementarity of the 16S rRNA penultimate stem with sequences downstream of the AUG destabilizes the plastid mRNAs. Nucleic Acids Res. 29, 970–975.
Lauxmann, M.A., Borsani, J., Osorio, S., Lombardo, V.A., Budde, C.O., Bustamante, C.A., Monti, L.L., Andreo, C.S., Fernie, A.R., Drincovich, M.F., Lara, M.V., 2014. Deciphering the metabolic pathways influencing heat and cold responses during post-harvest physiology of peach fruit. Plant Cell Environ. 37, 601–616.
Lopez-Calcagno, P.E., Fisk, S., Brown, K.L., Bull, S.E., South, P.F., Raines, C.A., 2019. Overexpressing the H-protein of the glycine cleavage system increases biomass yield

in glasshouse and field-grown transgenic tobacco plants. Plant Biotechnol. J 17, 141–151.
Luedemann, A., Strassburg, K., Erban, A., Kopka, J., 2008. TagFinder for the quantitative analysis of gas chromatography–mass spectrometry (GC-MS)-based metabolite profiling experiments. Bioinformatics 24, 732–737.
Luengwilai, K., Beckles, D.M., Roessner, U., Dias, D.A., Lui, V., Siriphanich, J., 2018. Identification of physiological changes and key metabolites coincident with postharvest internal browning of pineapple (Ananas comosus L.) fruit. Postharvest Biol. Technol. 137, 56–65.
Mi, J., Jia, K.P., Wang, J.Y., Al-Babili, S., 2018. A rapid LC-MS method for qualitative and quantitative profiling of plant apocarotenoids. Anal Chim Acta. 1035, 87–95.
Moreno, J.C., Cerda, A., Simpson, K., Lopez-Diaz, I., Carrera, E., Handford, M., Stange, C., 2016. Increased Nicotiana tabacum fitness through positive regulation of carotenoid, gibberellin and chlorophyll pathways promoted by Daucus carota lycopene beta-cyclase (Dclcyb1) expression. J. Exp. Bot. 678, 2325–2338. https://doi.org/10.1093/jxb/erw037.
Moreno, J.C., Martinez-Jaime, S., Kosmacz, M., Sokolowska, E.M., Schulz, P., Fischer, A., Luzarowska, U., Havaux, M., Skirycz, A., 2021a. A multi-OMICs approach sheds light on the higher yield phenotype and enhanced abiotic stress tolerance in tobacco lines expressing the carrot lycopene β-cyclase1 gene. Front. Plant Sci. 12.
Moreno, J.C., Mi, J., Agrawal, S., Kossler, S., Tureckova, V., Tarkowska, D., Thiele, W., Al-Babili, S., Bock, R., Schottler, M.A., 2020. Expression of a carotenogenic gene allows faster biomass production by redesigning plant architecture and improving photosynthetic efficiency in tobacco. Plant J. 103, 1967–1984.
Moreno, J.C., Mi, J., Alagoz, Y., Al-Babili, S., 2021b. Plant apocarotenoids: from retrograde signaling to interspecific communication. Plant J. 105, 351–375.
Murata, M., Nakai, Y., Kawazu, K., Ishizaka, M., Kajiwara, H., Abe, H., Takeuchi, K., Ichinose, Y., Mitsuhara, I., Mochizuki, A., Seo, S., 2019. Loliolide, a carotenoid metabolite, is a potential endogenous inducer of herbivore resistance. Plant Physiol. 179, 1822–1833.
Nambara, E., Marion-Poll, A., 2005. Abscisic acid biosynthesis and catabolism. Annu. Rev. Plant Biol. 56, 165–185.
Nitsch, L., Kohlen, W., Oplaat, C., Charnikhova, T., Cristescu, S., Michieli, P., Wolters-Arts, M., Bouwmeester, H., Mariani, C., Vriezen, W.H., Rieu, I., 2012. ABA-deficiency results in reduced plant and fruit size in tomato. J. Plant Physiol. 169, 878–883.
Niyogi, K.K., Truong, T.B., 2013. Evolution of flexible non-photochemical quenching mechanisms that regulate light harvesting in oxygenic photosynthesis. Curr. Opin. Plant Biol. 16, 307–314.
Ort, D.R., Merchant, S.S., Alric, J., Barkan, A., Blankenship, R.E., Bock, R., Croce, R., Hanson, M.R., Hibberd, J.M., Long, S.P., Moore, T.A., Moroney, J., Niyogi, K.K., Parry, M.A., Peralta-Yahya, P.P., Prince, R.C., Redding, K.E., Spalding, M.H., van Wijk, K.J., Vermaas, W.F., von Caemmerer, S., Weber, A.P., Yeates, T.O., Yuan, J.S., Zhu, X.G., 2015. Redesigning photosynthesis to sustainably meet global food and bioenergy demand. Proc. Natl. Acad. Sci. U. S. A. 112, 8529–8536.
Pang, Z., Chong, J., Li, S., Xia, J., 2020. MetaboAnalystR 3.0: toward an optimized workflow for global metabolomics. Metabolites 10.
Pareek, A., Dhankher, O.P., Foyer, C.H., 2020. Mitigating the impact of climate change on plant productivity and ecosystem sustainability. J. Exp. Bot. 71, 451–456.
Qin, G., Gu, H., Ma, L., Peng, Y., Deng, X.W., Chen, Z., Qu, L.J., 2007. Disruption of phytoene desaturase gene results in albino and dwarf phenotypes in Arabidopsis by impairing chlorophyll, carotenoid, and gibberellin biosynthesis. Cell Res. 17, 471–482.
Quinet, M., Angosto, T., Yuste-Lisbona, F.J., Blanchard-Gros, R., Bigot, S., Martinez, J.P., Lutts, S., 2019. Tomato fruit development and metabolism. Front. Plant Sci. 10, 1554.
Rittenberg, D., Foster, G.L., 1940. A new procedure for quantitative analysis BY isotope dilution, with application to the determination OF amino acids and fatty acids. J. Biol. Chem. 737–744.
Rodriguez-Concepcion, M., Avalos, J., Bonet, M.L., Boronat, A., Gomez-Gomez, L., Hornero-Mendez, D., Limon, M.C., Melendez-Martinez, A.J., Olmedilla-Alonso, B., Palou, A., Ribot, J., Rodrigo, M.J., Zacarias, L., Zhu, C., 2018. A global perspective on carotenoids: metabolism, biotechnology, and benefits for nutrition and health. Prog. Lipid Res. 70, 62–93.
Rodriguez-Villalon, A., Gas, E., Rodriguez-Concepcion, M., 2009a. Colors in the dark: a model for the regulation of carotenoid biosynthesis in etioplasts. Plant Signal. Behav. 4, 965–967.
Rodriguez-Villalon, A., Gas, E., Rodriguez-Concepcion, M., 2009b. Phytoene synthase activity controls the biosynthesis of carotenoids and the supply of their metabolic precursors in dark-grown Arabidopsis seedlings. Plant J. 60, 424–435.
Romer, S., Fraser, P.D., Kiano, J.W., Shipton, C.A., Misawa, N., Schuch, W., Bramley, P. M., 2000. Elevation of the provitamin A content of transgenic tomato plants. Nat. Biotechnol. 18, 666–669.
Roy, S.J., Negrao, S., Tester, M., 2014. Salt resistant crop plants. Curr. Opin. Biotechnol. 26, 115–124.
Salem, M.A., Juppner, J., Bajdzienko, K., Giavalisco, P., 2016. Protocol: a fast, comprehensive and reproducible one-step extraction method for the rapid preparation of polar and semi-polar metabolites, lipids, proteins, starch and cell wall polymers from a single sample. Plant Methods 12, 45.
Schaller, G.E., Bishopp, A., Kieber, J.J., 2015. The yin-yang of hormones: cytokinin and auxin interactions in plant development. Plant Cell 27, 44–63.
Shani, E., Salehin, M., Zhang, Y., Sanchez, S.E., Doherty, C., Wang, R., Mangado, C.C., Song, L., Tal, I., Pisanty, O., Ecker, J.R., Kay, S.A., Pruneda-Paz, J., Estelle, M., 2017. Plant stress tolerance requires auxin-sensitive aux/IAA transcriptional repressors. Curr. Biol. 27, 437–444.
Sharma, R., Priya, P., Jain, M., 2013. Modified expression of an auxin-responsive rice CC-type glutaredoxin gene affects multiple abiotic stress responses. Planta 238, 871–884.
Sheyhakinia, S., Bamary, Z., Einali, A., Valizadeh, J., 2020. The induction of salt stress tolerance by jasmonic acid treatment in roselle (Hibiscus sabdariffa L.) seedlings through enhancing antioxidant enzymes activity and metabolic changes. Biologia 75, 681–692.
Shi, H., Chen, L., Ye, T., Liu, X., Ding, K., Chan, Z., 2014. Modulation of auxin content in Arabidopsis confers improved drought stress resistance. Plant Physiol. Biochem. 82, 209–217.
Simkin, A.J., Lopez-Calcagno, P.E., Davey, P.A., Headland, L.R., Lawson, T., Timm, S., Bauwe, H., Raines, C.A., 2017. Simultaneous stimulation of sedoheptulose 1,7-bisphosphatase, fructose 1,6-bisphophate aldolase and the photorespiratory glycine decarboxylase-H protein increases CO2 assimilation, vegetative biomass and seed yield in Arabidopsis. Plant Biotechnol. J 15, 805–816.
Simkin, A.J., McAusland, L., Headland, L.R., Lawson, T., Raines, C.A., 2015. Multigene manipulation of photosynthetic carbon assimilation increases CO2 fixation and biomass yield in tobacco. J. Exp. Bot. 66, 4075–4090.
Simura, J., Antoniadi, I., Siroka, J., Tarkowska, D., Strnad, M., Ljung, K., Novak, O., 2018. Plant hormonomics: multiple phytohormone profiling by targeted metabolomics. Plant Physiol. 177, 476–489.
Singh, M., Kumar, J., Singh, S., Singh, V.P., Prasad, S.M., 2015. Roles of osmoprotectants in improving salinity and drought tolerance in plants: a review. Rev. Environ. Sci. Biotechnol. 14, 407–426.
South, P.F., Cavanagh, A.P., Liu, H.W., Ort, D.R., 2019. Synthetic glycolate metabolism pathways stimulate crop growth and productivity in the field. Science 363.
Talon, M., Koornneef, M., Zeevaart, J.A., 1990. Endogenous gibberellins in Arabidopsis thaliana and possible steps blocked in the biosynthetic pathways of the semidwarf ga4 and ga5 mutants. Proc. Natl. Acad. Sci. U. S. A. 87, 7983–7987.
Tietz, S., Hall, C.C., Cruz, J.A., Kramer, D.M., 2017. NPQ(T) : a chlorophyll fluorescence parameter for rapid estimation and imaging of non-photochemical quenching of excitons in photosystem-II-associated antenna complexes. Plant Cell Environ. 40, 1243–1255.
Timm, S., Wittmiss, M., Gamlien, S., Ewald, R., Florian, A., Frank, M., Wirtz, M., Hell, R., Fernie, A.R., Bauwe, H., 2015. Mitochondrial dihydrolipoyl dehydrogenase activity shapes photosynthesis and photorespiration of Arabidopsis thaliana. Plant Cell 27, 1968–1984.
Toumi, I., Moschou, P.N., Paschalidis, K.A., Bouamama, B., Ben Salem-Fnayou, A., Ghorbel, A.W., Mliki, A., Roubelakis-Angelakis, K.A., 2010. Abscisic acid signals reorientation of polyamine metabolism to orchestrate stress responses via the polyamine exodus pathway in grapevine. J. Plant Physiol. 167, 519–525.
Tran, L.S., Urao, T., Qin, F., Maruyama, K., Kakimoto, T., Shinozaki, K., Yamaguchi-Shinozaki, K., 2007. Functional analysis of AHK1/ATHK1 and cytokinin receptor histidine kinases in response to abscisic acid, drought, and salt stress in Arabidopsis. Proc. Natl. Acad. Sci. U. S. A. 104, 20623–20628.
Ueguchi-Tanaka, M., Nakajima, M., Katoh, E., Ohmiya, H., Asano, K., Saji, S., Hongyu, X., Ashikari, M., Kitano, H., Yamaguchi, I., Matsuoka, M., 2007. Molecular interactions of a soluble gibberellin receptor, GID1, with a rice DELLA protein, SLR1, and gibberellin. Plant Cell 19, 2140–2155.
Valero, D., Martinez-Romero, D., Serrano, M., 2002. The role of polyamines in the improvement of the shelf life of fruit. Trends Food Sci. Technol. 13, 228–234.
Wang, J., Song, L., Gong, X., Xu, J.F., Li, M.H., 2020. Functions of jasmonic acid in plant regulation and response to abiotic stress. Int. J. Mol. Sci. 21.
Wang, J.Y., Haider, I., Jamil, M., Fiorilli, V., Saito, Y., Mi, J., Baz, L., Kountche, B.A., Jia, K.P., Guo, X., Balakrishna, A., Ntui, V.O., Reinke, B., Volpe, V., Gojobori, T., Blilou, I., Lanfranco, L., Bonfante, P., Al-Babili, S., 2019. The apocarotenoid metabolite zaxinone regulates growth and strigolactone biosynthesis in rice. Nat. Commun. 10, 810.
Wurbs, D., Ruf, S., Bock, R., 2007. Contained metabolic engineering in tomatoes by expression of carotenoid biosynthesis genes from the plastid genome. Plant J. 49, 276–288.
Xu, P., Chukhutsina, V.U., Nawrocki, W.J., Schansker, G., Bielczynski, L.W., Lu, Y., Karcher, D., Bock, R., Croce, R., 2020. Photosynthesis without beta-carotene. Elife 9.
Xu, Y., 2016. Envirotyping for deciphering environmental impacts on crop plants. Theor. Appl. Genet. 129, 653–673.
Yoshida, T., Mogami, J., Yamaguchi-Shinozaki, K., 2014. ABA-dependent and ABA-independent signaling in response to osmotic stress in plants. Curr. Opin. Plant Biol. 21, 133–139.
Zhang, Y., Li, Y., Hassan, M.J., Li, Z., Peng, Y., 2020. Indole-3-acetic acid improves drought tolerance of white clover via activating auxin, abscisic acid and jasmonic acid related genes and inhibiting senescence genes. BMC Plant Biol. 20, 150.

Supporting Information

Supplementary Figures

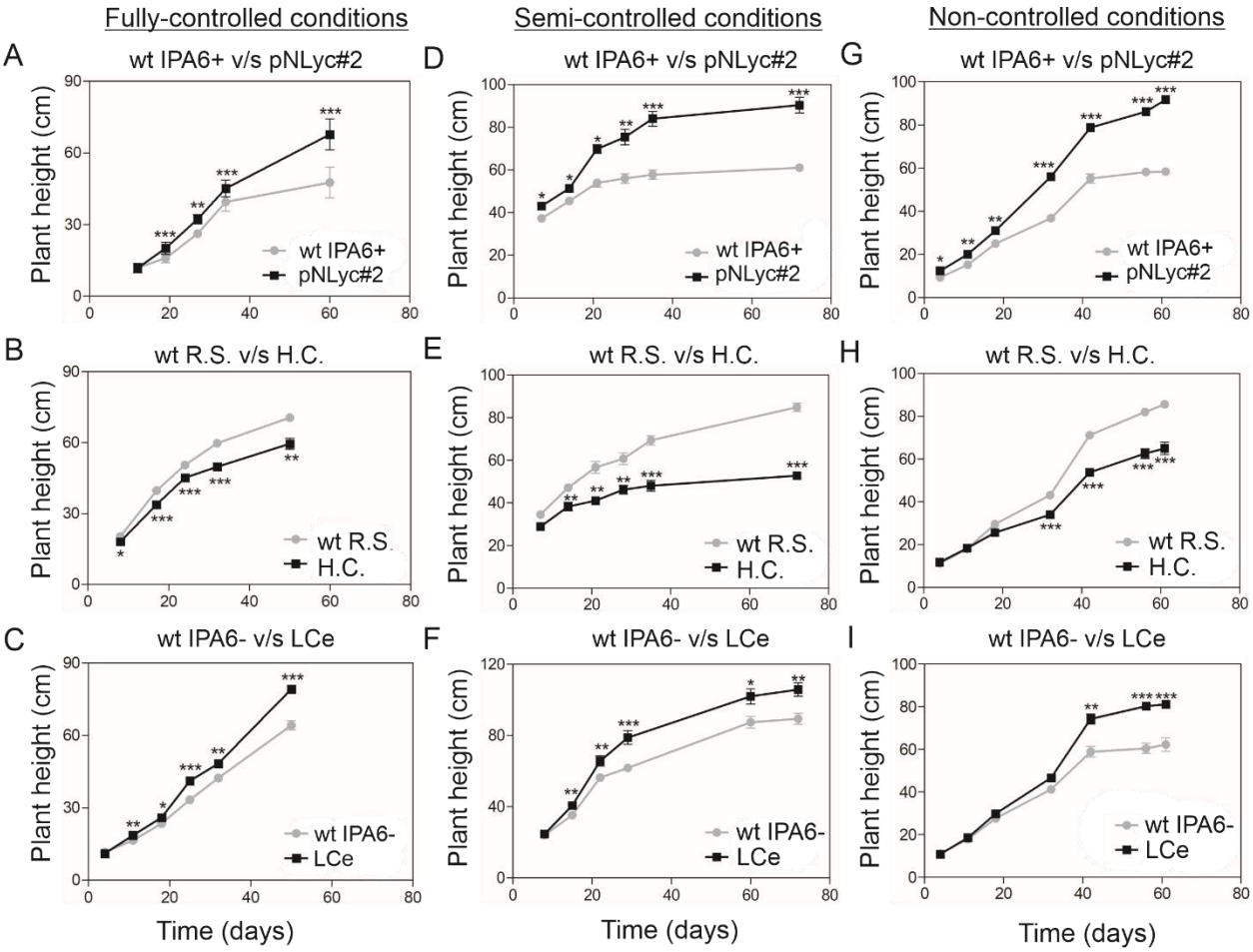

Fig. S1. Growth rate of wild type and transgenic tomato lines growing under controlled and non-controlled conditions. (A-I) Tomato plant growth under fully- (plant chamber/530 and 53 µmol m^{-2} s^{-1} red and white light respectively, 16/8 h photoperiod, 70 % relative humidity and 24 °C/**A-C**), semi- (greenhouse/average light intensity: 170-380 µmol m^{-2} s^{-1}, maximum light intensity: 1200 µmol $m^{-2}s^{-1}$ and 24 °C/**D-F**), and non-controlled conditions (polytunnel/natural climate conditions during spring-summer 2019 in Potsdam, Germany/**G-I**). Plant height for wild type (IPA6+, R.S., and IPA6-) and transgenic (pNLyc#2, H.C., and LCe) lines was recorded at different time points during their development. Data points and error bar represent the means and the ±SEM (*n*=10) in each environmental condition. Non-paired two-tailed Student t-test was performed to compare each transgenic line with the wild type (*: $p < 0.05$, **: $p < 0.001$, ***: $p < 0.0001$). wt: wild type; R.S.: Red Setter; H.C.: high carotene; LCe: lycopene β-cyclase from Erwinia.

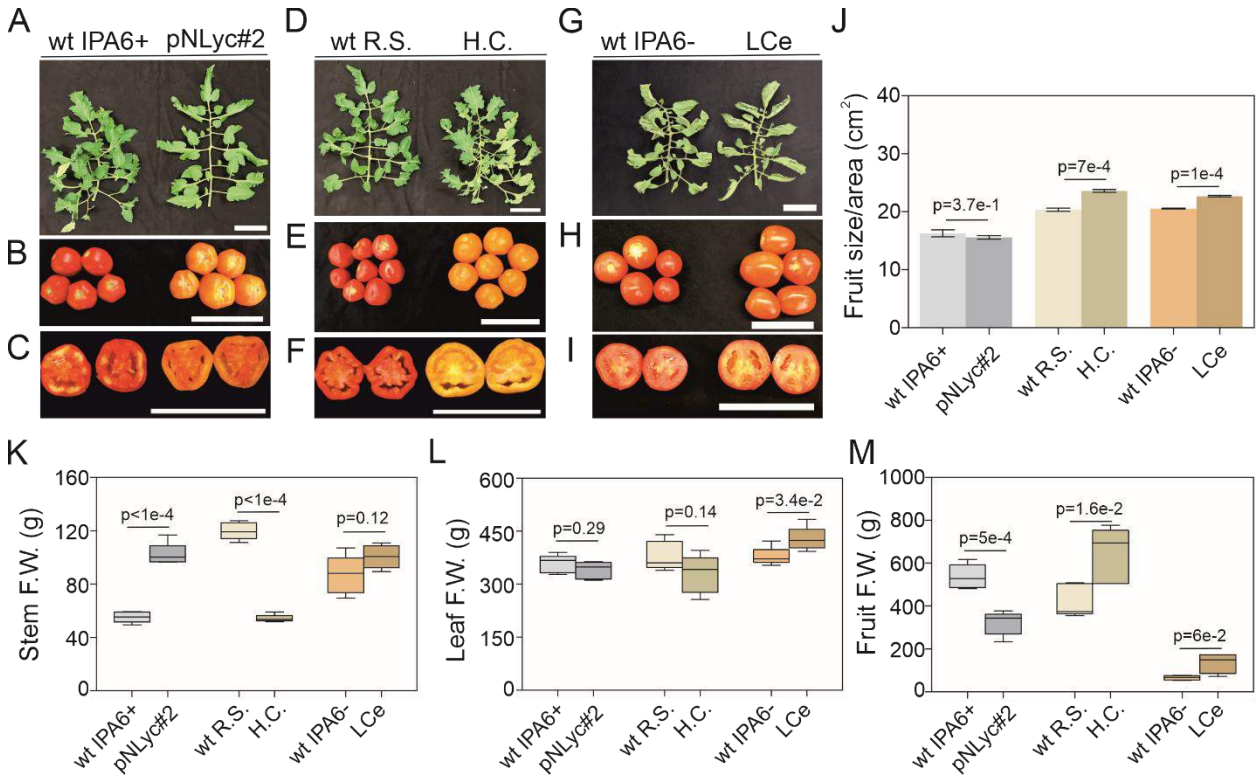

Fig. S2. Phenotype and fresh weight quantification in *LCYB* tomatoes grown in the greenhouse. (A-I) Tomato (16-week-old) wild type (IPA6+, R.S., and IPA6-) and transgenic (pNLyc#2, H.C., and LCe) plants grown under semi-controlled conditions in the greenhouse. A comparison between the seventh leaf, five fruits, and fruit flesh of wt and transgenic lines is shown. (**J**) Tomato fruit size of wild type and transgenic lines was measured in fully ripened fruits at the same developmental stage from 16-week-old tomato plants (*n*=3) grown under greenhouse conditions. **(K-M)** Tomato fresh weight (F.W.; stem, leaf, and fruit) of wild type and transgenic lines. Non-paired two-tailed Student t-test was performed to compare transgenic lines with the wild type (*n*=5-7) wt: wild type; R.S.: Red Setter; H.C.: high carotene; LCe: lycopene β-cyclase from Erwinia. Scale bar: 10 cm.

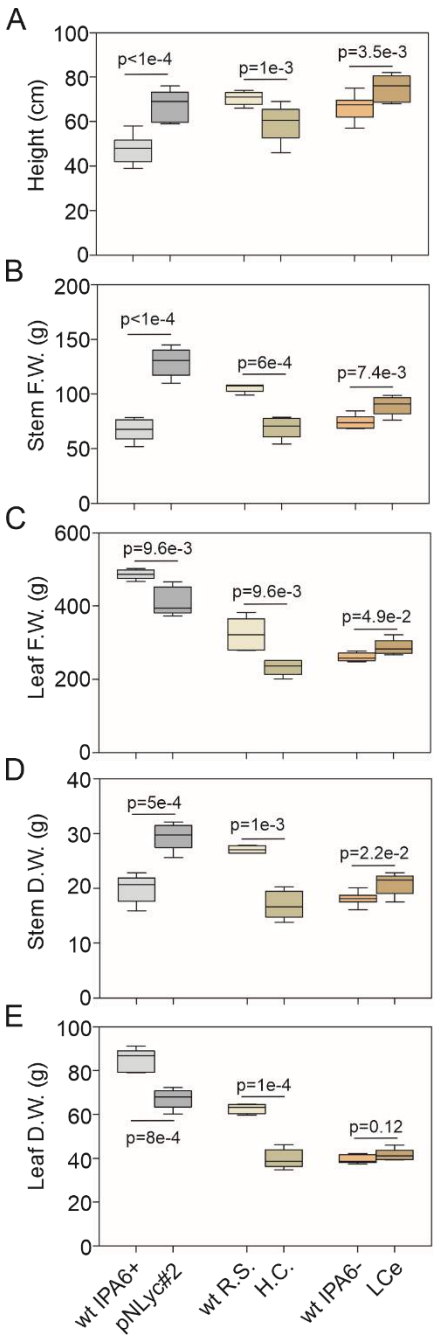

Fig. S3. Biomass production of wild type and transgenic tomatoes grown under fully controlled conditions. (A-E) Plant height and biomass production (fresh and dry weight of leaf and stem) in wild type (IPA6+, R.S., and IPA6-) and transgenic (pNLyc#2, H.C., and LCe) tomato plants grown under fully controlled conditions for 60 days. Non-paired two-tailed Student t-test was performed to compare transgenic lines with the wild type (*n*=5). wt: wild type; R.S.: Red Setter; H.C.: high carotene; LCe: lycopene β-cyclase from Erwinia.

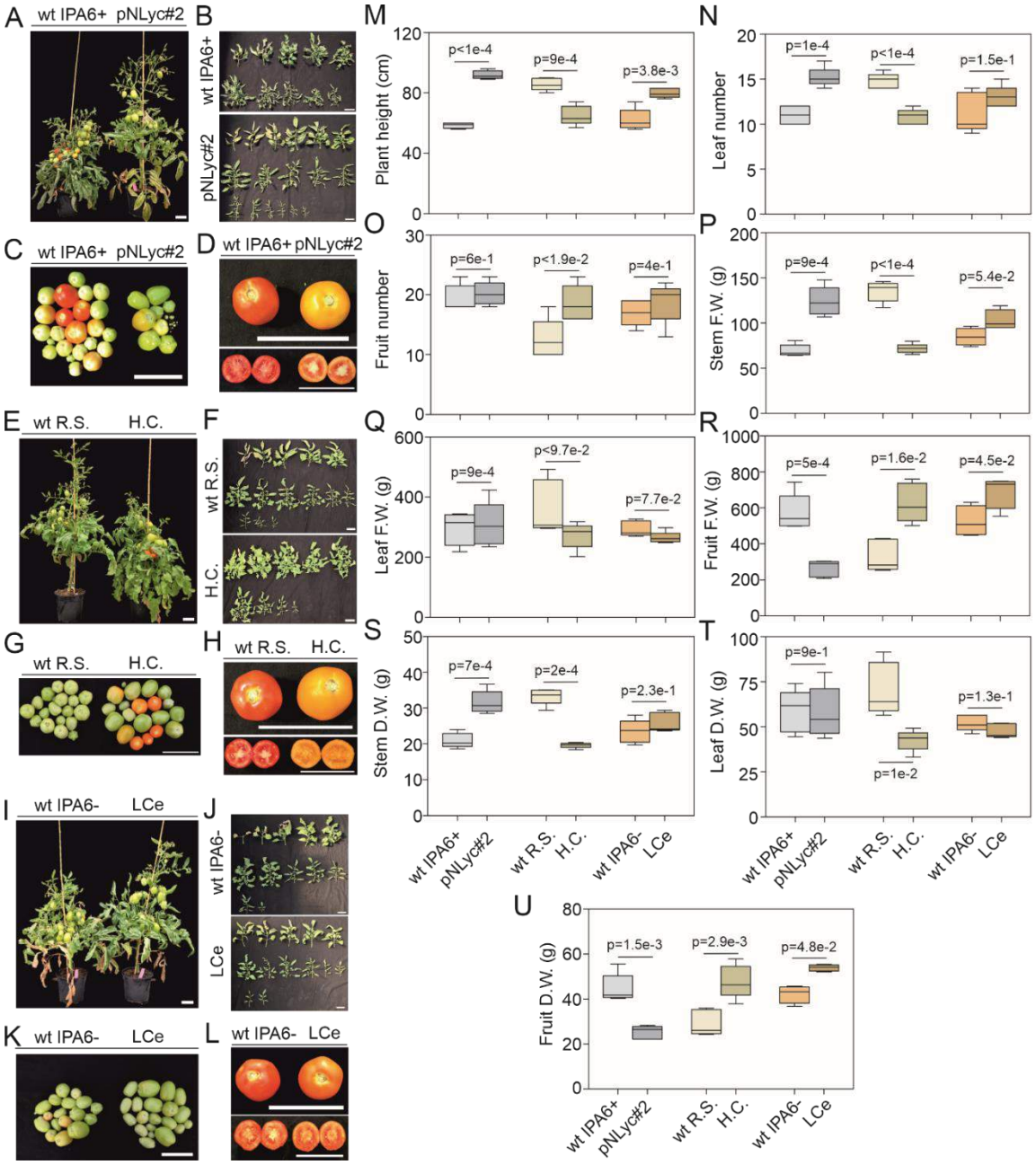

Fig. S4. Biomass production of wild type and transgenic tomatoes grown under non-controlled conditions in the polytunnel. (A-L) Tomato (12-week-old) plant height **(A, E, I)**, leaf series **(B, F, J)**, and total fruit production **(C, G, K)** measurements, in wild type (IPA6+, R.S., and IPA6-) and transgenic lines (pNLyc#2, H.C., and LCe). Tomato fruit and flesh from 16-week-old tomato plants is shown for wild type and transgenic lines **(D, H, L).** Plant height **(M)**, leaf **(N)**, and fruit number **(O)**, in wild type and transgenic lines. Biomass quantification in fresh **(P-R)** and dry weight **(S-U)** of the stem, leaf and fruits from wild type and transgenic tomato lines. Non-paired two-tailed Student t-test was performed to compare transgenic lines with the wild type (for plant height, leaf, and fruit number n=10 biological replicates; for biomass n=5 biological replicates). wt: wild type; R.S.: Red Setter; H.C.: high carotene; LCe: lycopene β-cyclase from Erwinia.

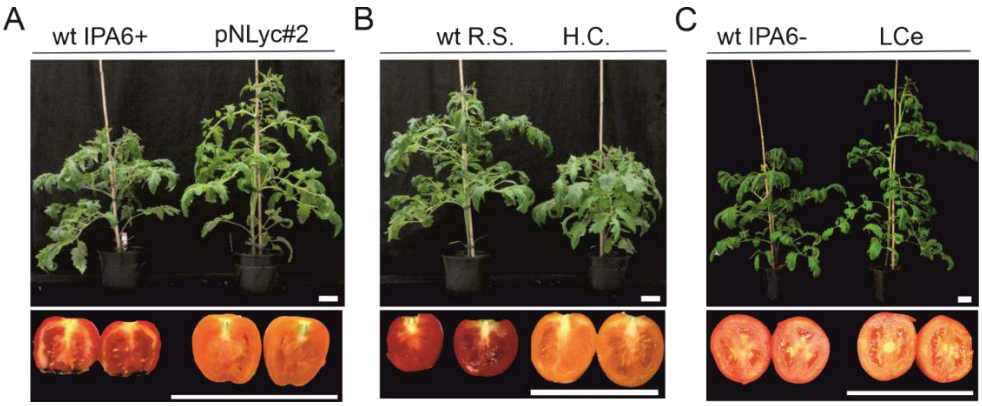

Fig. S5. Tomato leaves and fruits from wild type and transgenic tomatoes grown under semi-controlled conditions in the greenhouse. (A-C) Six-week-old wild type (IPA6+, R.S., and IPA6-) and transgenic lines (pNLyc#2, H.C., and LCe) grown under semi-controlled conditions in the greenhouse. Fruits were harvested from 16-week-old tomato plants. wt: wild type; R.S.: Red Setter; H.C.: high carotene; LCe: lycopene β-cyclase from Erwinia. Scale bar: 10 cm.

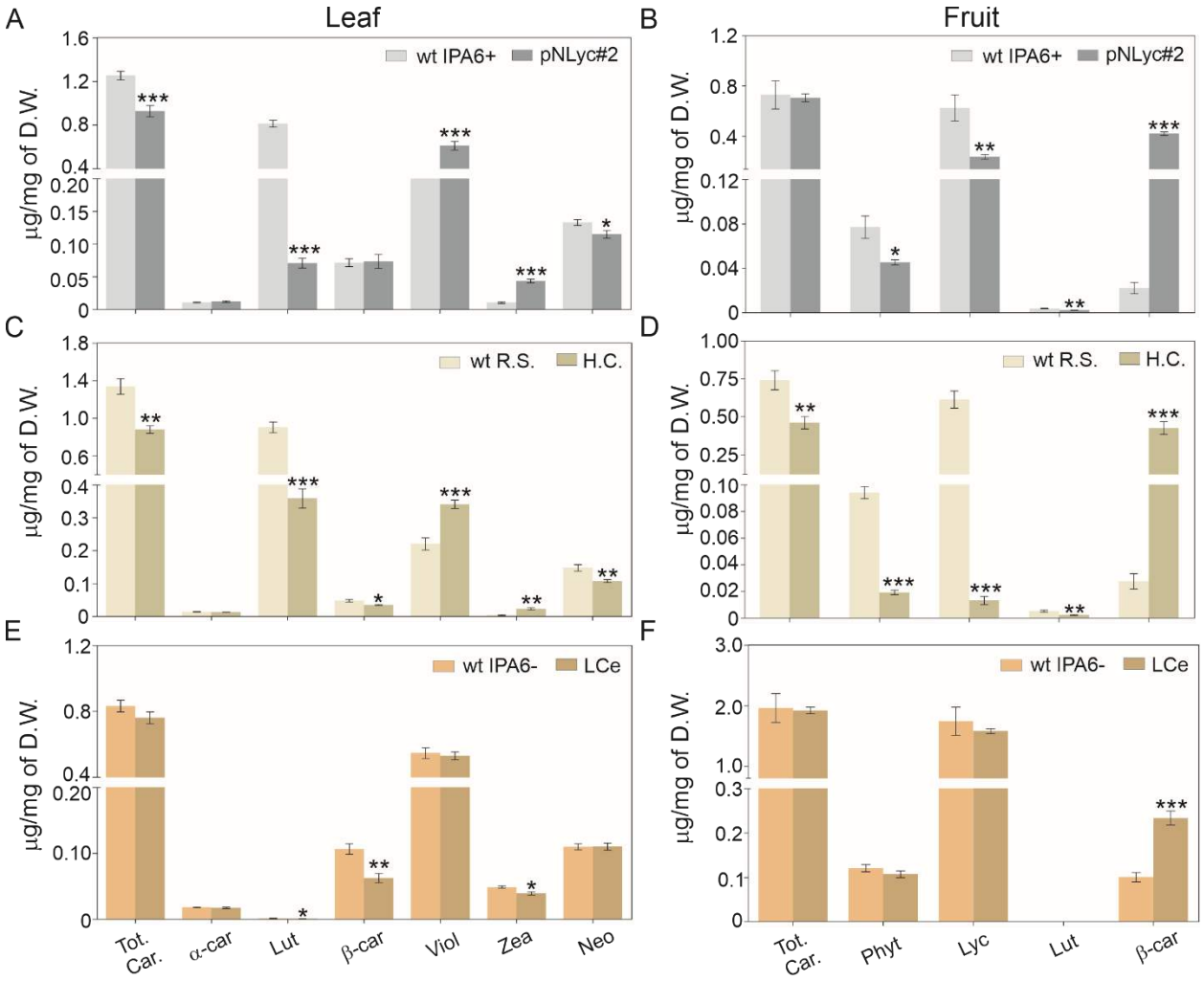

Fig. S6. Carotenoid quantification in wild type and transgenic tomatoes. (A-B) Carotenoid quantification in leaf and fruit of six-week-old wild type IPA6+ and pNLyc#2 tomato plants. **(C-D)** Carotenoid quantification in leaf and fruit in six-week-old wild type R.S. and H.C. tomato plants. **(E-F)** Carotenoid quantification in leaf and fruit in six-week-old wild type IPA6- and LCe tomato plants. Columns and bars represent the means and the ±SEM (*n*=5). Non-paired two-tailed Student t-test was performed to compare transgenic lines with the wild type. *: $p < 0.05$, **: $p < 0.01$ ***: $p < 0.005$. wt: wild type; R.S.: Red Setter; H.C.: high carotene; LCe: lycopene β-cyclase from Erwinia; Viol: violaxanthin; Neo: neoxanthin; Lut; lutein; Zea: zeaxanthin; car: carotene; Phyt: phytoene; Lyc: lycopene; Tot. car.: total carotenoids.

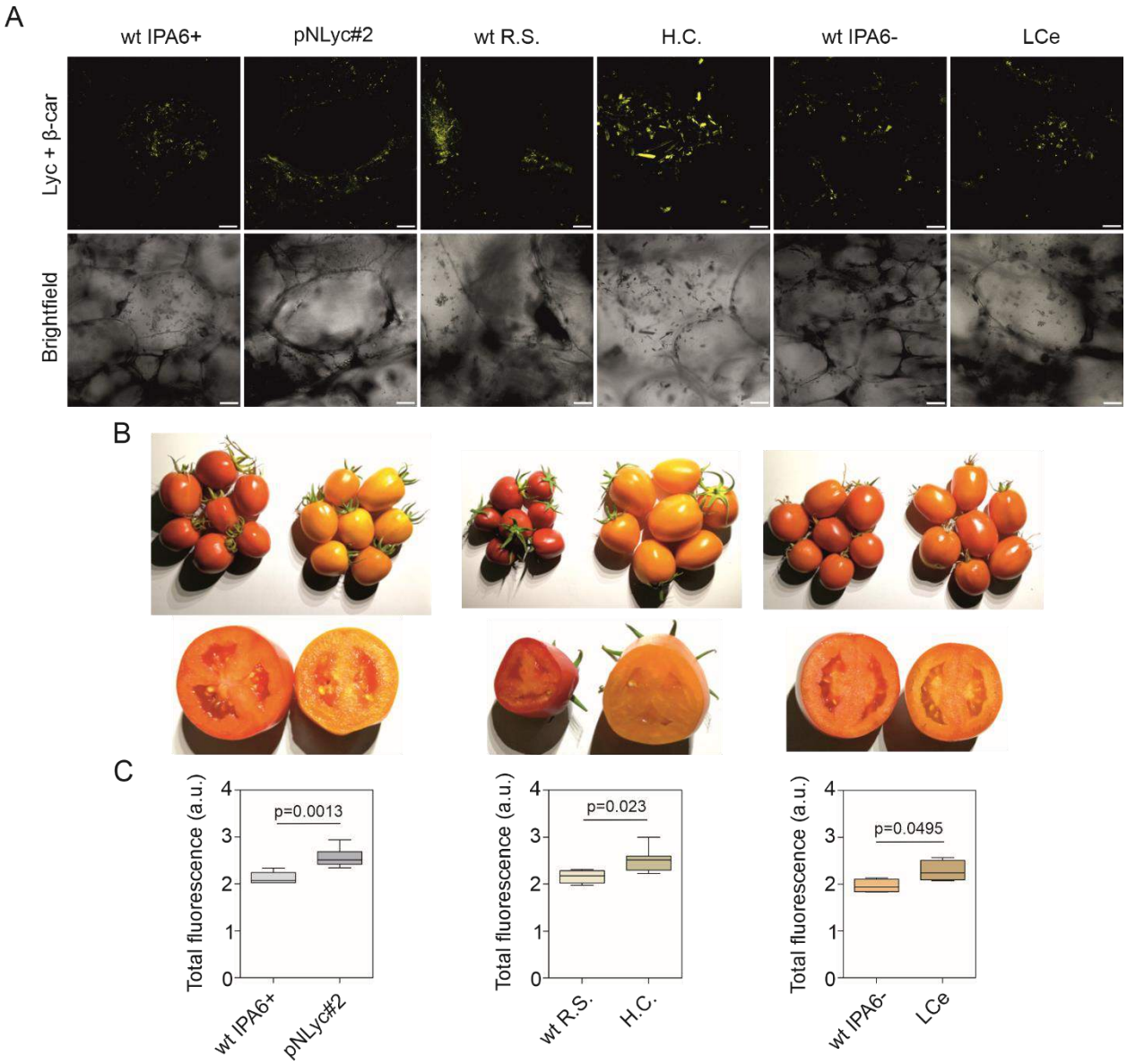

Fig. S7. Microscopy analysis in wild type and transgenic tomatoes. (A) Microscopy analysis of carotenoid (lycopene/Lyc and β-carotene/β-car) content in the fruit of wild type (IPA6+, R.S., and IPA6-) and transgenic lines (pNLyc#2, H.C., and LCe; n = 3). **(B)** Tomato fruits harvested from 12-week-old tomato wild type and transgenic lines. **(C)** Carotenoid fluorescence quantification (wavelength 400-550 nm) of carotenoids (lycopene and β-carotene). Ten images from 3 different fruits were used for the quantification of the fluorescence. Non-paired two-tailed Student t-test was performed to compare transgenic lines with the wild type (n = 3-5). wt: wild type; R.S.: Red Setter; H.C.: high carotene; LCe: lycopene β-cyclase from Erwinia. Scale bar: 50 μM.

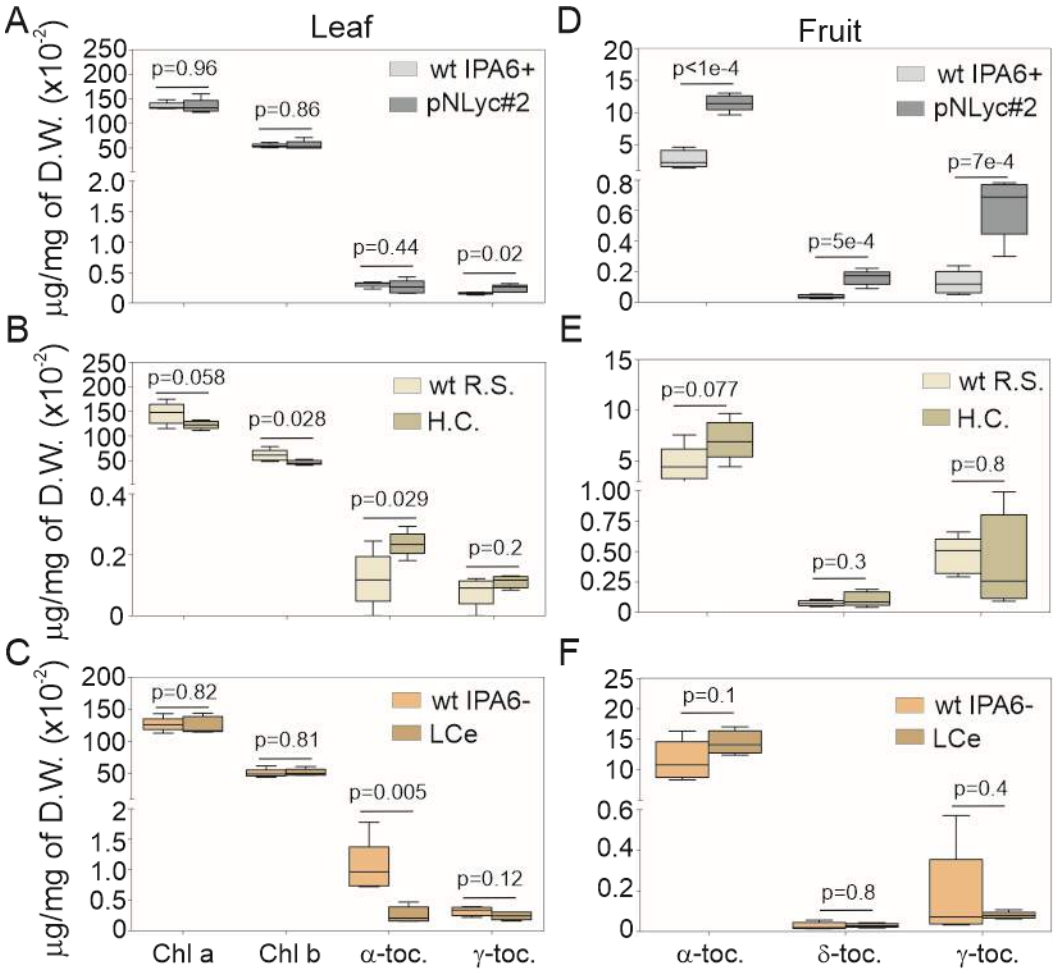

Fig. S8. Chlorophyll and tocopherol quantification in wild type and transgenic tomatoes. (A-C) Chlorophyll and tocopherol composition in leaf. **(D-F)** Tocopherol composition in fruit. Leaf samples were collected from the 5th leaf of each of the five biological replicates used per line (6-week-old plants). Fully-ripen fruits were collected from 16-week-old tomato plants (from five different biological replicates, each biological replicate comprising a pool of 3 fruits). Tomato plants were grown under greenhouse conditions (16 h/8 h day/night regime, 450-800 µmol photons m^{-2} s^{-1}/combination of artificial and sun light, 24 °C, and 65 % relative humidity). Pigments were extracted and quantified by HPLC according to Emiliani et al., 2018. Non-paired two-tailed Student t-test was performed to compare transgenic lines with the wild type. wt: wild type; R.S.: Red Setter; H.C.: high carotene; LCe: lycopene β-cyclase from Erwinia; Chl: chlorophyll; Toc: tocopherol.

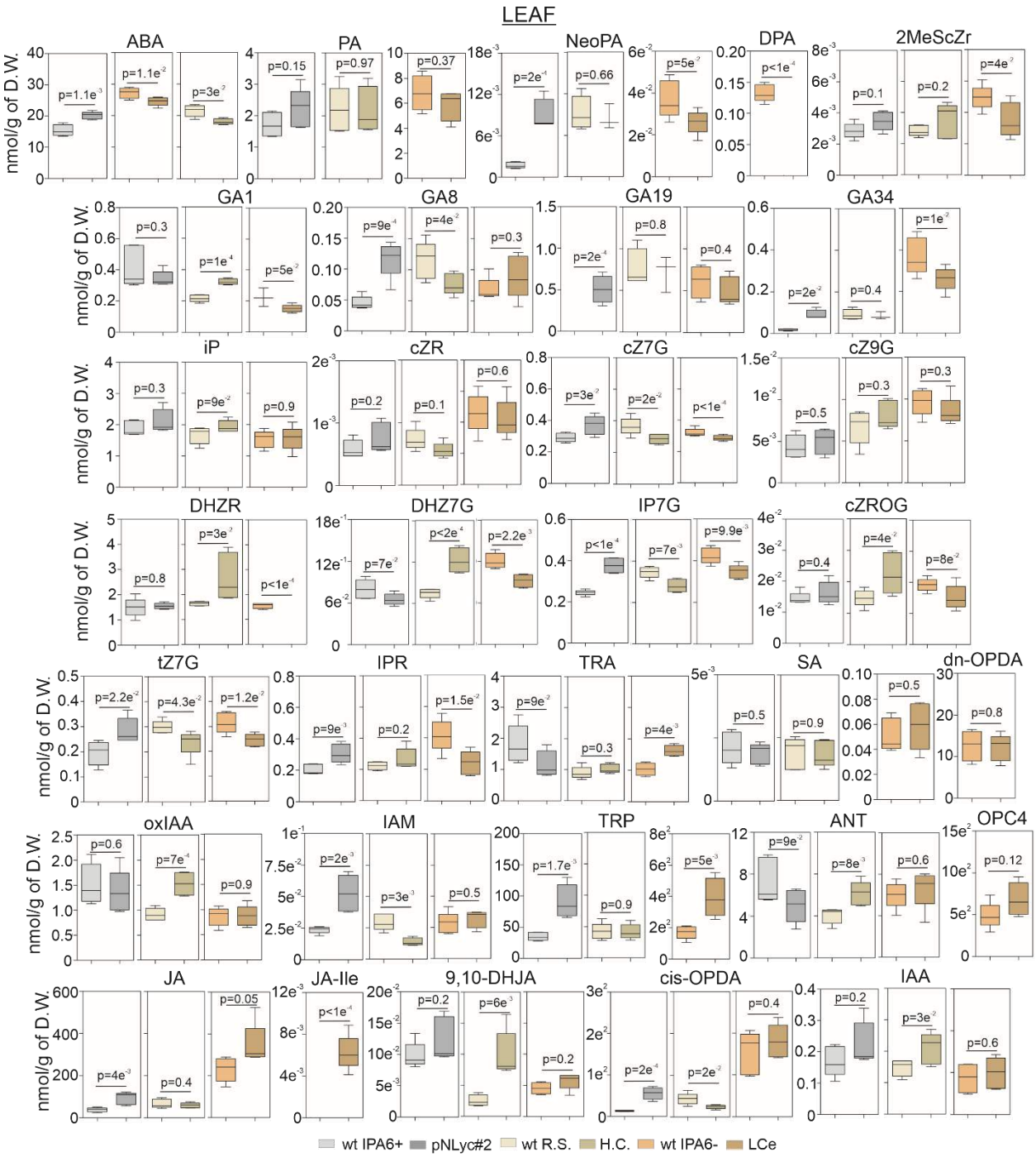

Fig. S9. Hormone profiling in leaf. Hormones, metabolites, and catabolites measured in leaves of wild type (IPA6+, R.S., and IPA6-) and transgenic tomato lines (pNLyc#2, H.C., and LCe) by LC-MS/MS. Non-paired two-tailed Student t-test was performed to compare transgenic lines with the wild type (n = 5). wt: wild type; R.S.: Red Setter; H.C.: high carotene; LCe: lycopene β-cyclase from Erwinia. For abbreviations see **Table S4**.

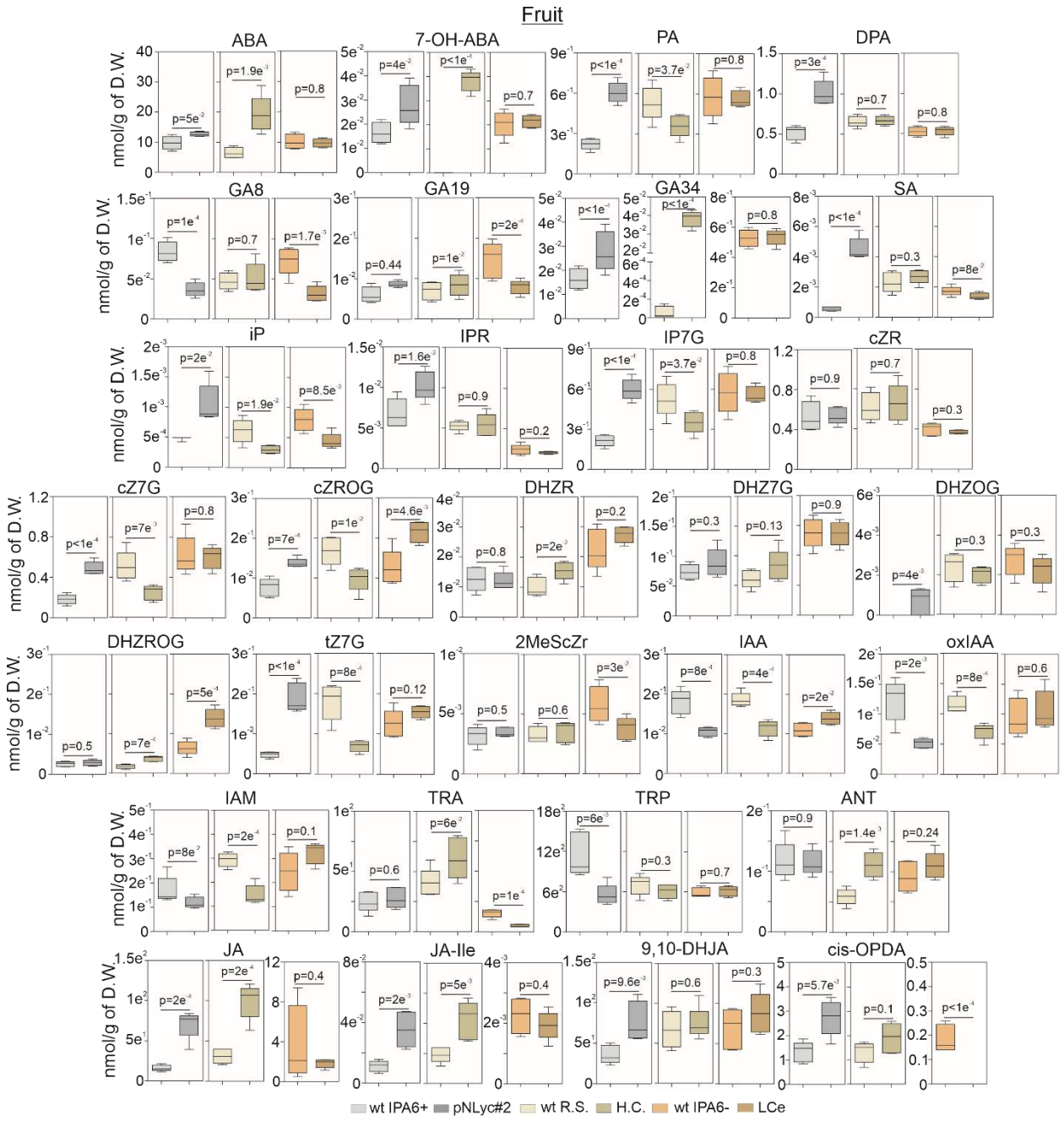

Fig. S10. Hormone profiling in fruit. Hormones, metabolites, and catabolites measured in fruits of wild type (IPA6+, R.S., and IPA6-) and transgenic tomato lines (pNLyc#2, H.C., and LCe) by LC-MS/MS. Non-paired two-tailed Student t-test was performed to compare transgenic lines with the wild type (n = 5). wt: wild type; R.S.: Red Setter; H.C.: high carotene; LCe: lycopene β-cyclase from Erwinia. For abbreviations see **Table S4**.

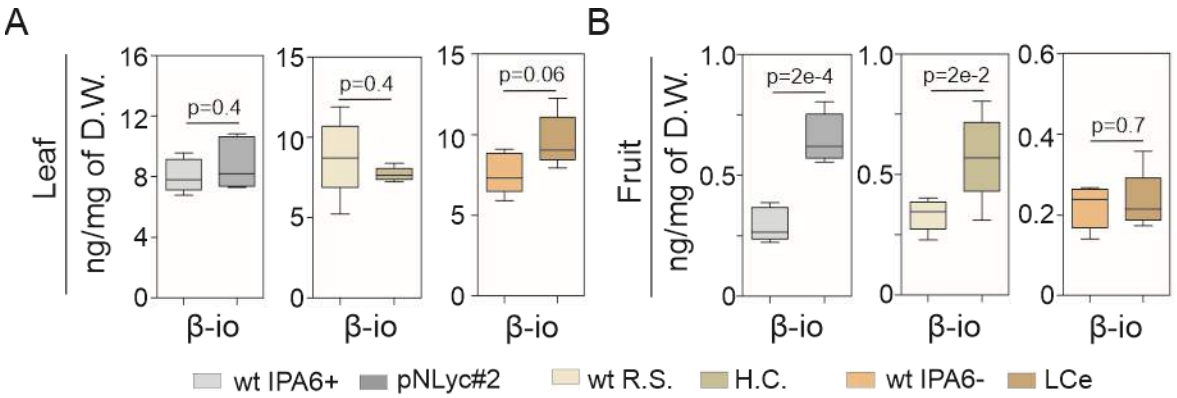

Fig. S11. β-ionone accumulation in leaf and fruits of tomato *LCYB*-expressing lines. (A-B) β-ionone content measured in leaf (A) and fruits (B) of wild type (IPA6+, R.S., and IPA6-) and transgenic tomato lines (pNLyc#2, H.C., and LCe). Non-paired two-tailed Student t-test was performed to compare transgenic lines with the wild type ($p<0.05$; $n=5$). wt: wild type; R.S.: Red Setter; H.C.: high carotene; LCe: lycopene β-cyclase from Erwinia.

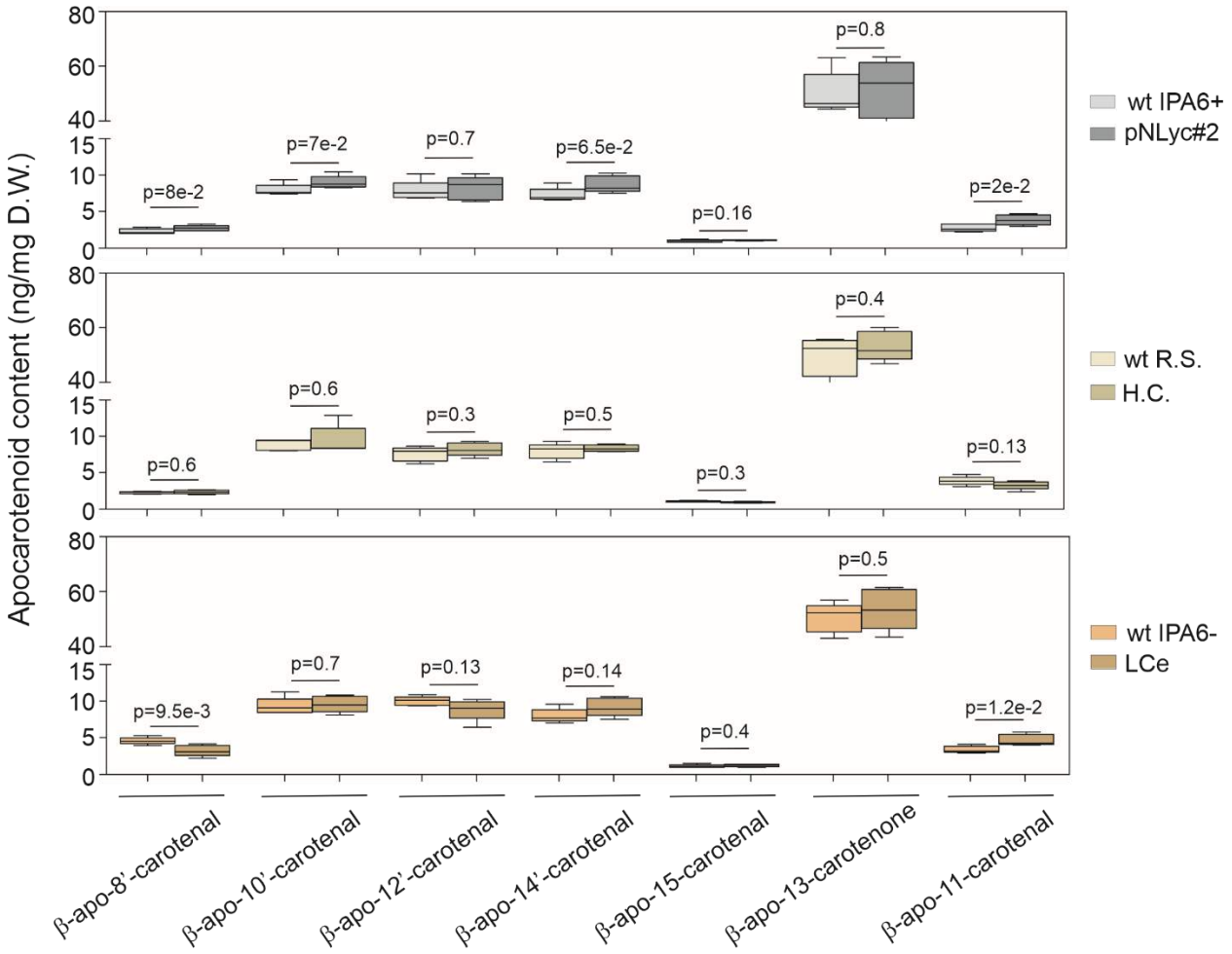

Fig. S12. Apocarotenoid profiling in leaf of tomato *LCYB*-expressing lines. Non-hydroxylated apocarotenoid species were quantified from six-week-old tomato leaves of wild type (IPA6+, R.S., and IPA6-) and transgenic lines (pNLyc#2, H.C., and LCe). Non-paired two-tailed Student t-test was performed to compare transgenic lines with the wild type ($p<0.05$; $n=5$). wt: wild type; R.S.: Red Setter; H.C.: high carotene; LCe: lycopene β-cyclase from Erwinia.

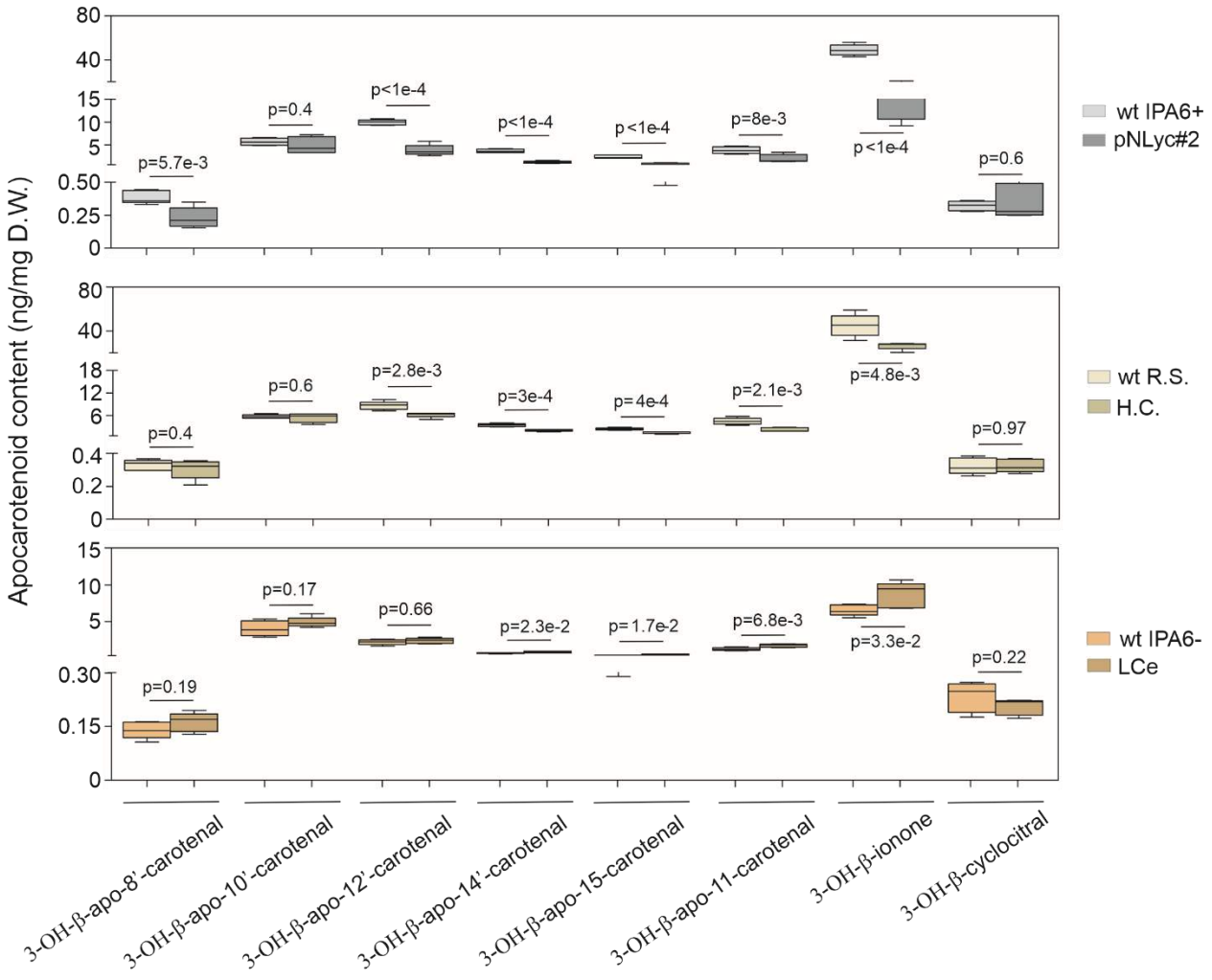

Fig. S13. Hydroxylated-apocarotenoid profiling in leaf of tomato *LCYB*-expressing lines. Hydroxylated apocarotenoid species were quantified from six-week-old tomato leaves of wild type (IPA6+, R.S., and IPA6-) and transgenic lines (pNLyc#2, H.C., and LCe). Non-paired two-tailed Student t-test was performed to compare transgenic lines with the wild type ($p<0.05$; $n=5$). wt: wild type; R.S.: Red Setter; H.C.: high carotene; LCe: lycopene β-cyclase from Erwinia.

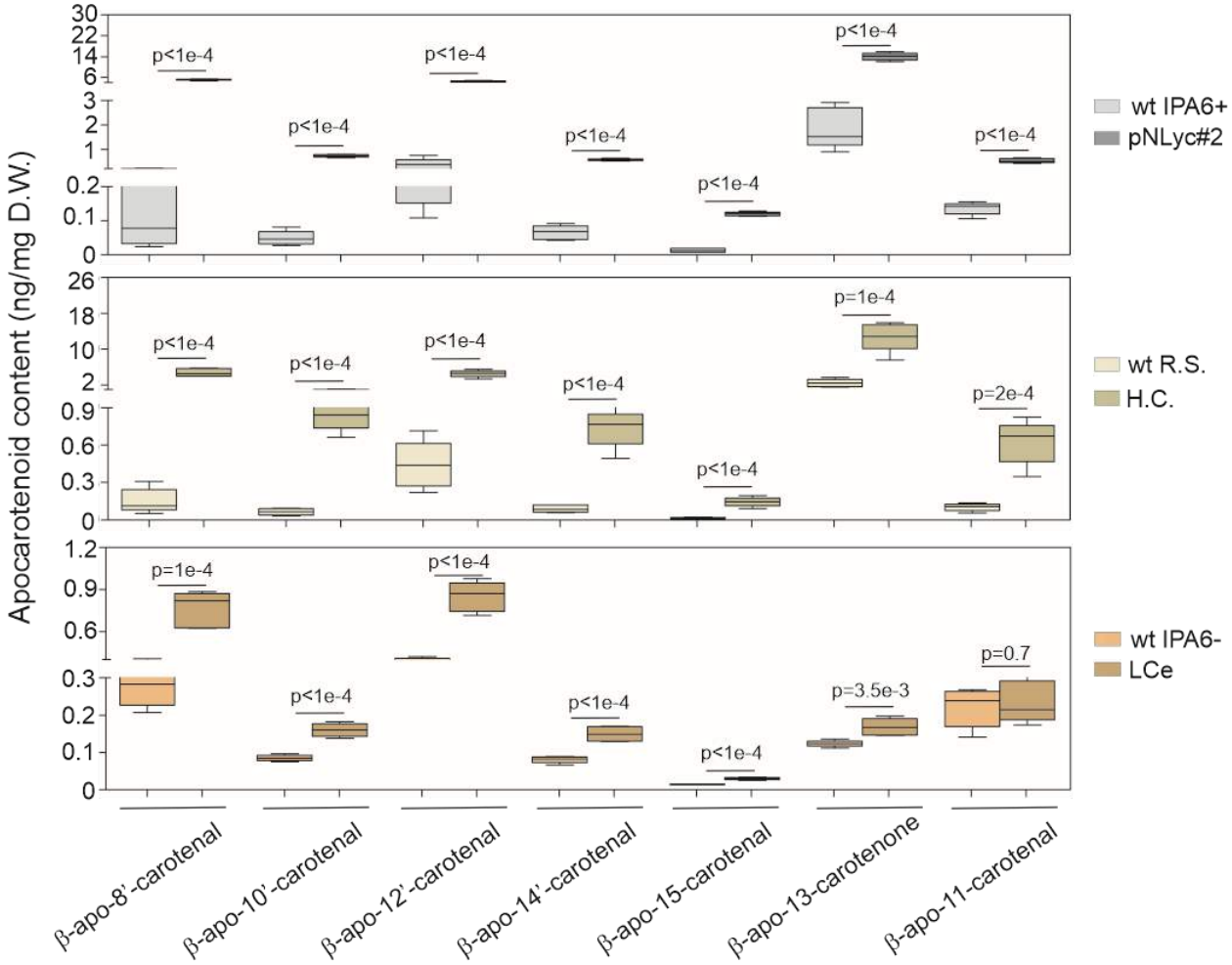

Fig. S14. Apocarotenoid profiling in fruits of tomato *LCYB*-expressing lines. Non-hydroxylated apocarotenoid species were quantified from six-week-old tomato leaves of wild type (IPA6+, R.S., and IPA6-) and transgenic lines (pNLyc#2, H.C., and LCe). Non-paired two-tailed Student t-test was performed to compare transgenic lines with the wild type ($p<0.05$; $n=5$). wt: wild type; R.S.: Red Setter; H.C.: high carotene; LCe: lycopene β-cyclase from Erwinia.

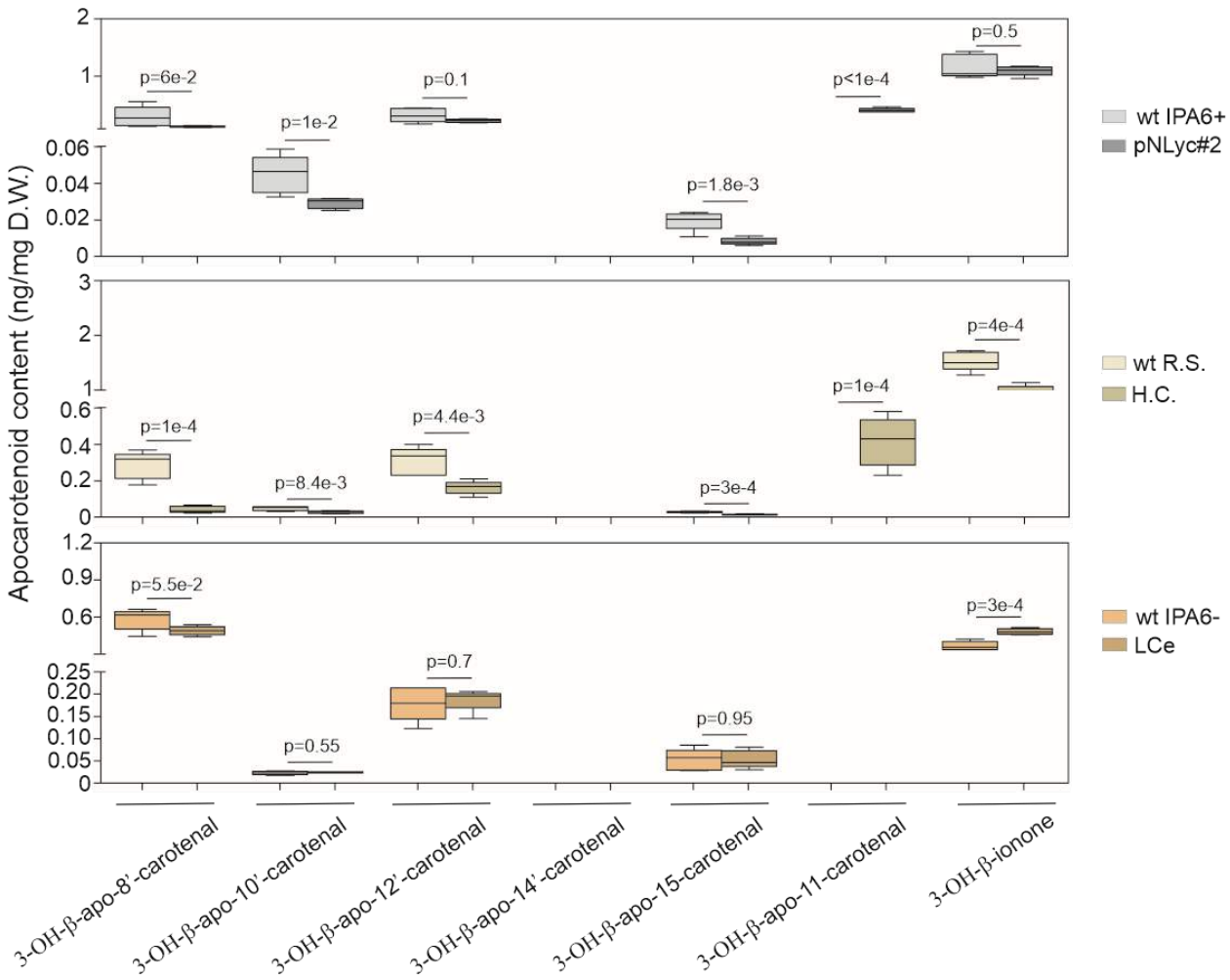

Fig. S15. Hydroxylated-apocarotenoid profiling in fruits of tomato *LCYB*-expressing lines. Hydroxylated apocarotenoid species were quantified from 16-week-old tomato fruits of wild type (IPA6+, R.S., and IPA6-) and transgenic lines (pNLyc#2, H.C., and LCe). Non-paired two-tailed Student t-test was performed to compare transgenic lines with the wild type ($p<0.05$; $n = 5$). wt: wild type; R.S.: Red Setter; H.C.: high carotene; LCe: lycopene β-cyclase from Erwinia.

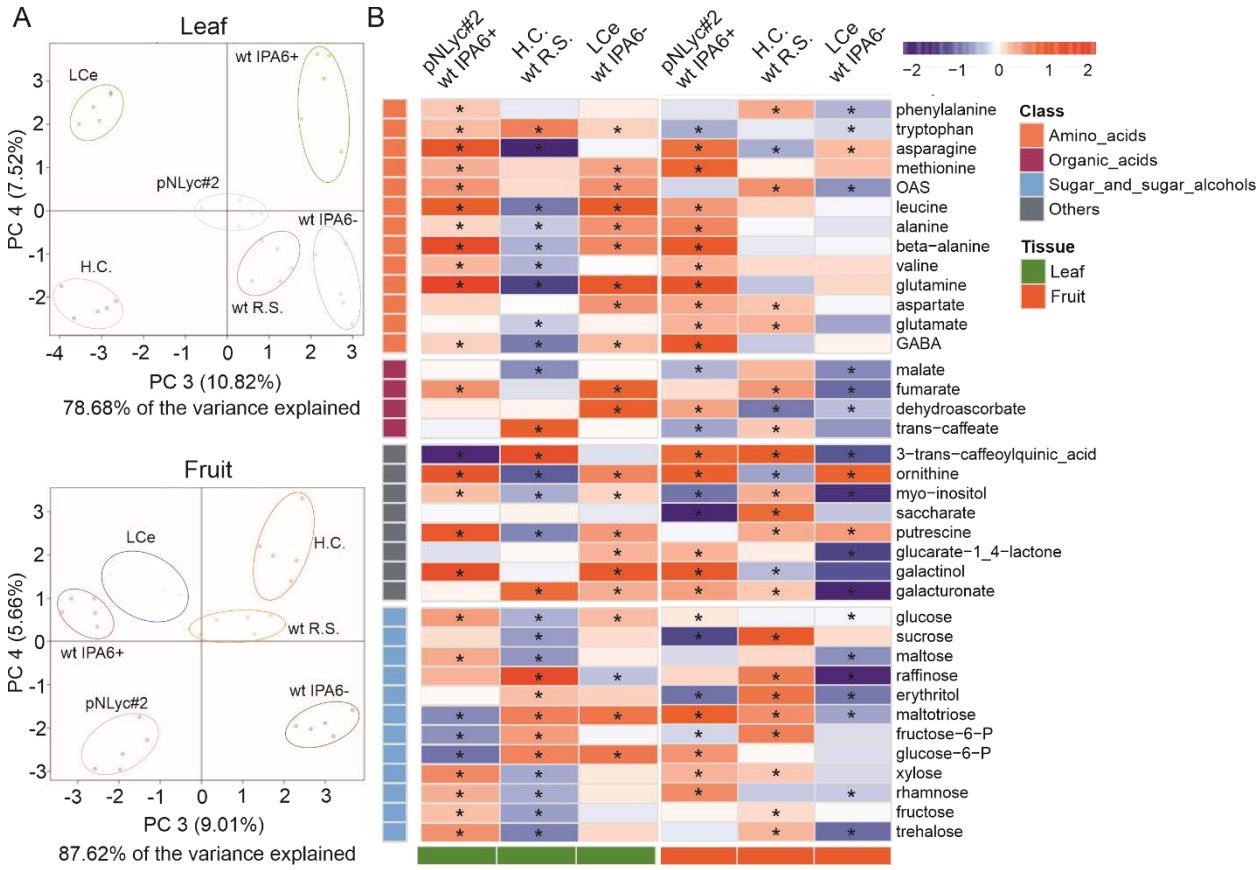

Fig. S16. Metabolite profiling in *LCYB*-expressing tomato lines. (A) Principal component analysis (PCA) of metabolite samples profiled in leaves and fruits of wild type (IPA6+, R.S., and IPA6-) and *LCYB* transgenic lines (pNLyc#2, H.C., and LCe). **(B)** Heatmap representing the metabolic changes occurring in leaf and fruits of tomato wild type (IPA6+, R.S., and IPA6-) and *LCYB* transgenic lines (pNLyc#2, H.C., and LCe). Non-paired Student t-test was performed to compare each transgenic line with their wild type ($p<0.05$; $n=5$). Changes are shown as log2 fold change between the transgenic lines and their respective wild-type controls.

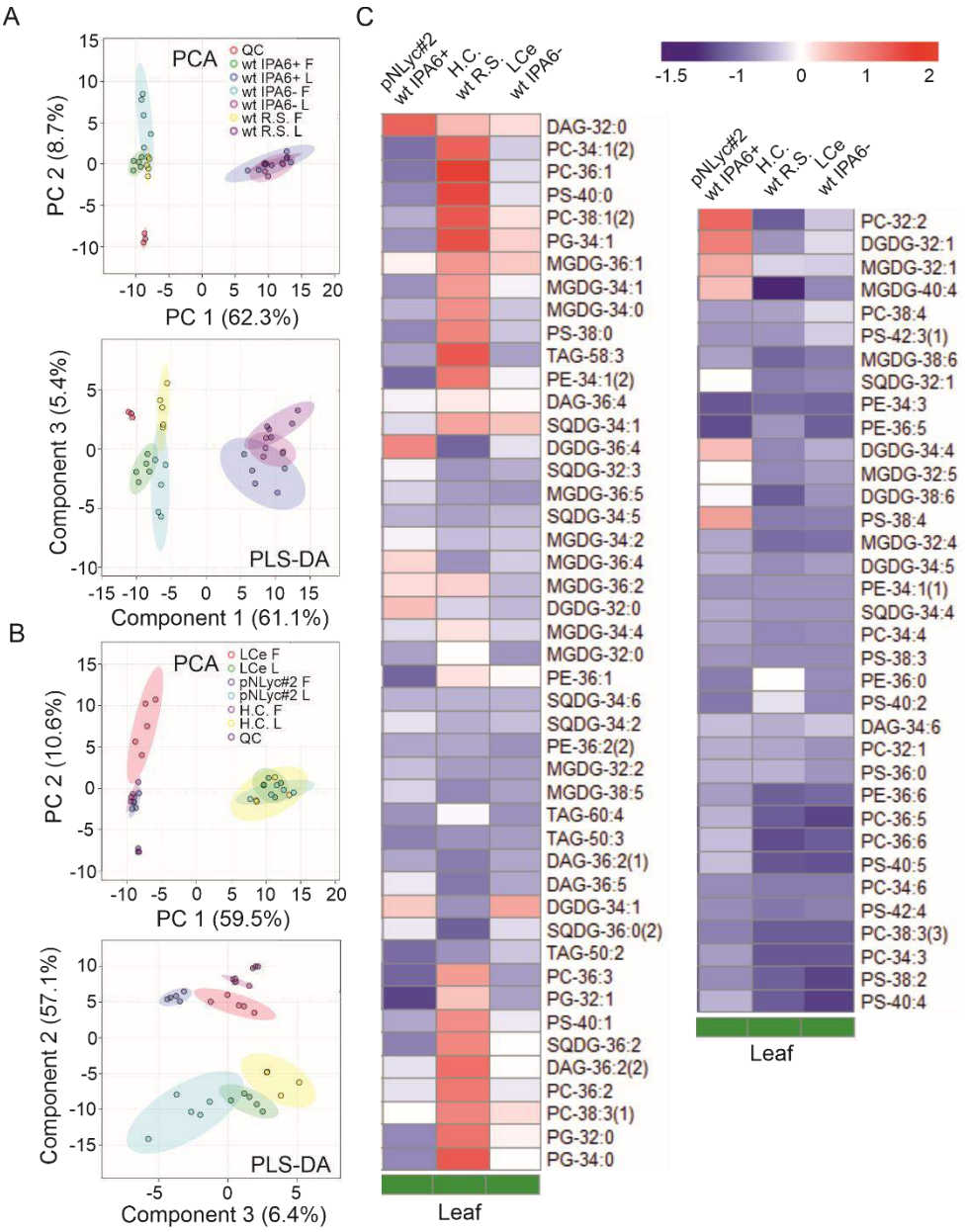

Fig. S17. Lipid profile in leaves of transgenic *LCYB* tomato lines. Principal component and partial least-squares discriminant analyses (PCA and PLS-DA, respectively) of metabolite samples profiled in leaves and fruits of **(A)** wild type (IPA6+, R.S., and IPA6-) and **(B)** *LCYB* transgenic lines (pNLyc#2, H.C., and LCe). **(C)** The Heatmap represents the leaf lipid abundance ratios calculated among the *LCYB* transgenic lines (pNLyc#2, H.C., and LCe) and the respective wild types (IPA6+, R.S., and IPA6-). The Wilcoxon's test was performed to compare transgenic lines with their wild types (n=5) and no significant differences were observed. Changes are shown as log2 fold change between the transgenic lines and their respective wild-type controls. DAG: diacylglycerol; DGDG: di-galactosyldiacylglycerol; MGDG: mono-galactosyldiacylglycerol; PC: phosphatidylcholine; PE: phosphatidylethanolamine; PG: phosphatidylglycerol; PS: phosphatidylserine; SQDG: sulfoquinovosyl diacylglycerol; TAG: triacylglycerol.

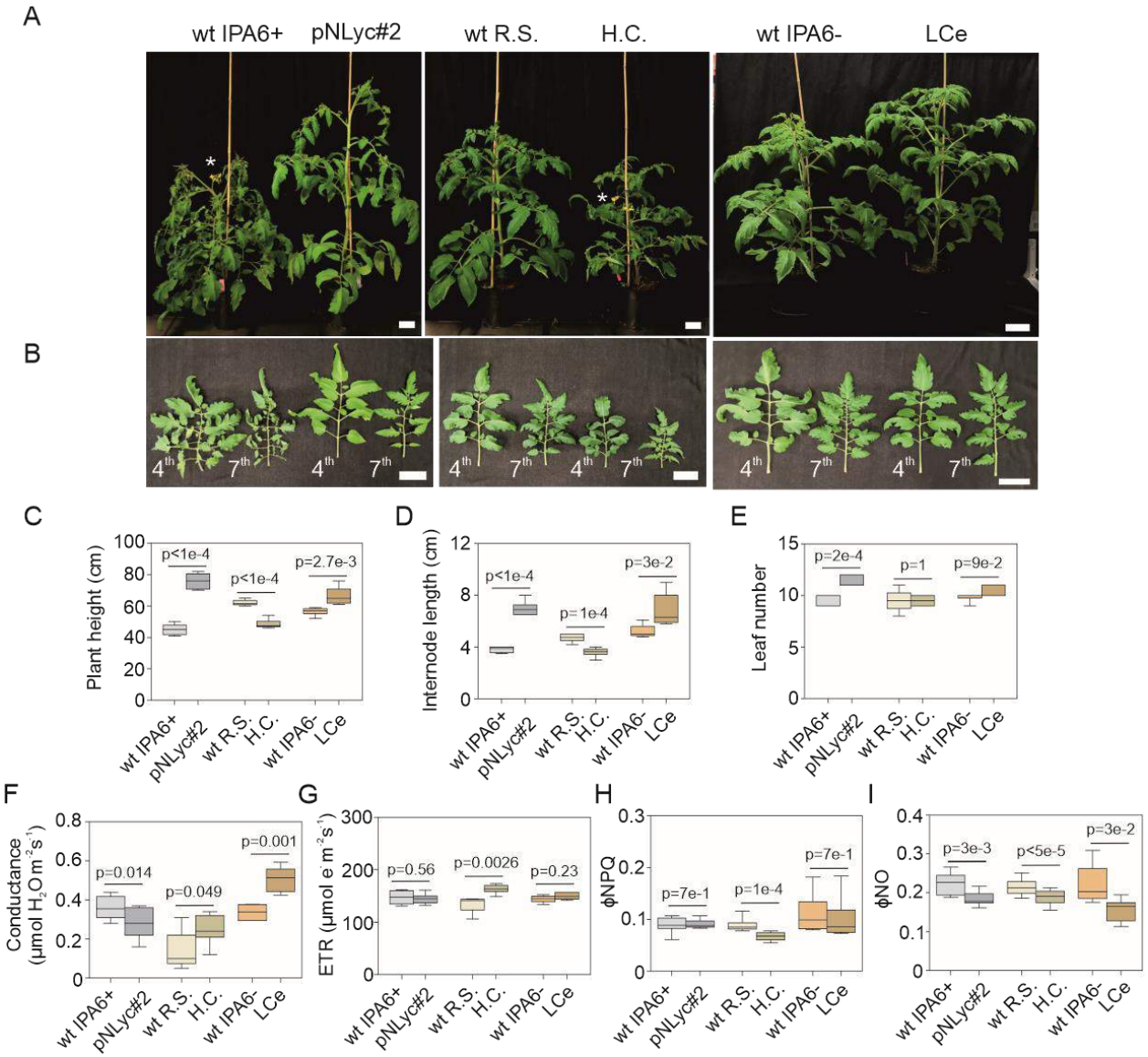

Fig. S18. Plant phenotype and physiological and photosynthetic parameters of *LCYB*-expressing tomatoes. (A) Six-week-old wild type (IPA6+, R.S., and IPA6-) and transgenic lines (pNLyc#2, H.C., and LCe) grown under semi-controlled conditions in the greenhouse. Asterisks in white show the presence of flowers. **(B)** Leaf phenotype of the 4th and the 7th leaves of wild type and transgenic lines (both were measured and showed similar results; results from the 7th leaf are shown). **(C)** Plant height. **(D)** Internode length. **(E)** Leaf number. **(F)** Conductance. **(G)** Electron transport rate (ETR). Conductance and ETR were measured with a LiCor instrument. **(H)** ΦNPQ. **(I)** ΦNO. Non-paired two-tailed Student t-test was performed to compare transgenic lines with the wild type (*n*=4-6). wt: wild type; R.S.: Red Setter; H.C.: high carotene; LCe: lycopene β-cyclase from Erwinia. Scale bar: 10 cm.

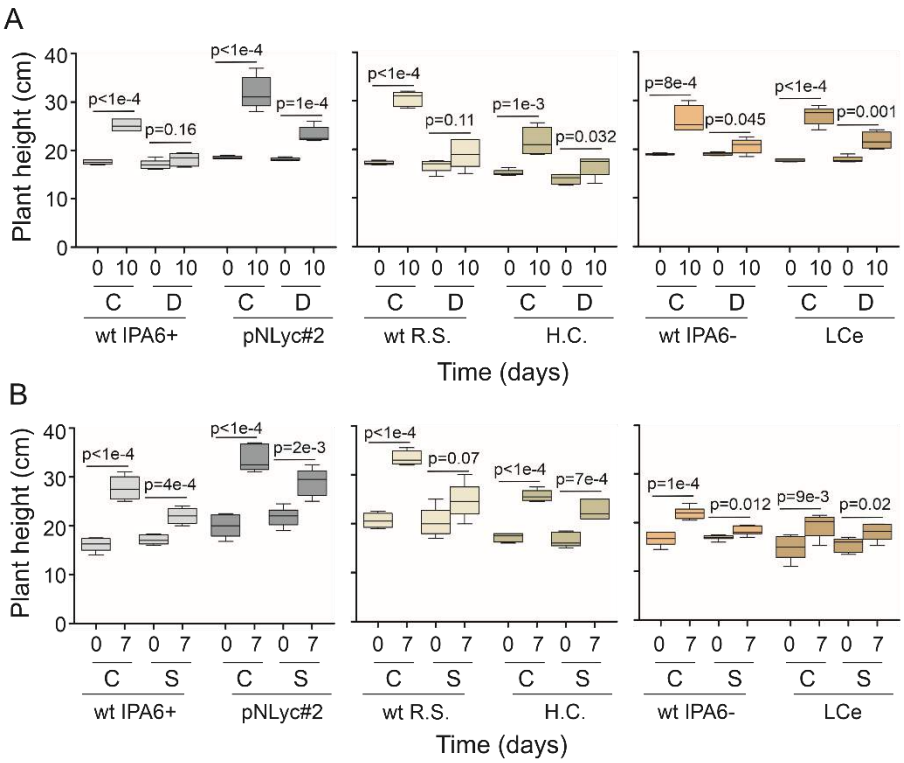

Fig. S19. Drought and salt tolerance in tomato plants. (A) Three-week old wild type (IPA6+, R.S., and IPA6-) and transgenic lines (pNLyc#2, H.C., and LCe) were subjected to control (water) and drought treatments in the greenhouse. The watering was stopped for 10 days in the drought-stressed plants, and the control plants were watered every day with increasing amounts of water (see Material and Methods). **(B)** Three-week old wild type and transgenic lines were subjected to control (water) and salt treatments in the greenhouse. Tomato plants were watered with 200 mM NaCl or water (100-200 mL) for seven days and afterwards seven days only with water. Plant height was recorded before and after drought and salt treatments. Non-paired two-tailed Student t-test was performed to compare transgenic lines with the wild type (*n*=5-6). wt: wild type; R.S.: Red Setter; H.C.: high carotene; LCe: lycopene β-cyclase from Erwinia. Scale bar: 10 cm.

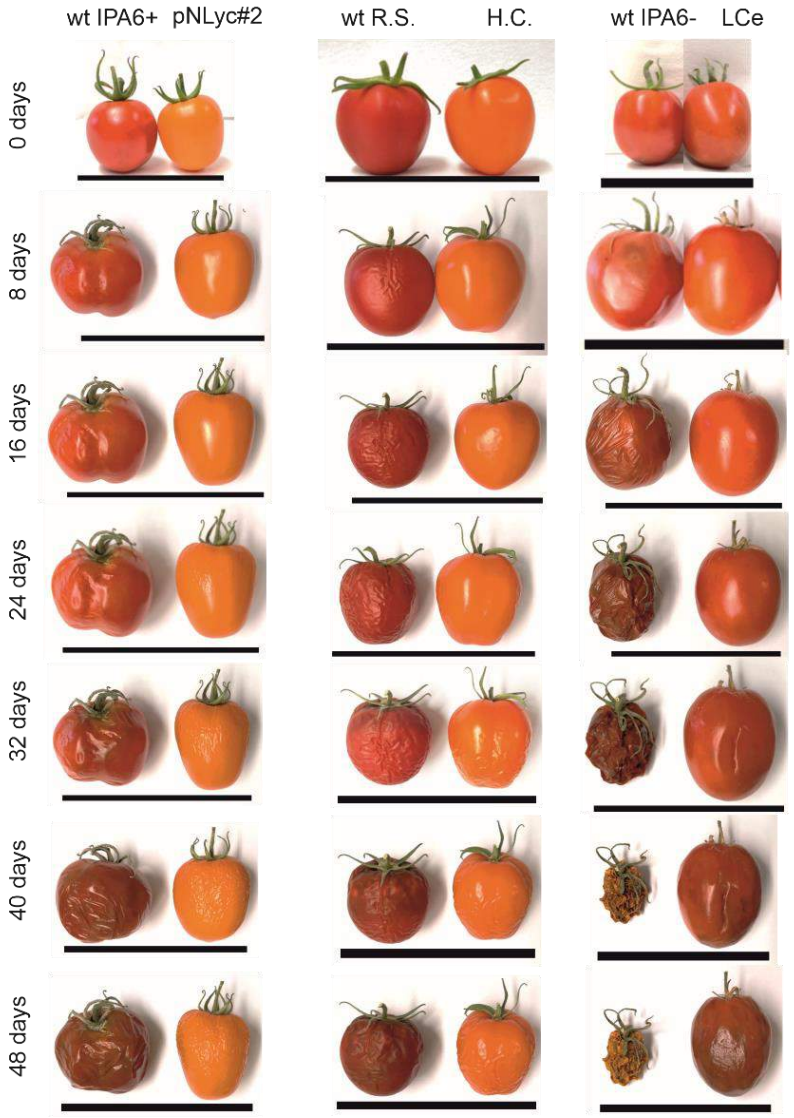

Fig. S20. Tomato fruit shelf life. Tomato fruits from wild type (IPA6+, R.S., and IPA6-) and transgenic lines (pNLyc#2, H.C., and LCe) were harvested from three months old tomato plants and stored at room temperature in the laboratory. Tomato fruits were recorded at 0, 8, 16, 24, 32, 40, and 48 days after harvesting. wt: wild type; R.S.: Red Setter; H.C.: high carotene; LCe: lycopene β-cyclase from Erwinia. Scale bar: 10 cm.

Table S1. Summary of the nuclear and transplastomic LCYB tomato lines used in this work.

Line	Cultivar	Gene	Organism	Transformation	Seed generation	Reference
pNLyc#2	IPA6+Lut	*LCYB*	Daffodil	Plastid	T4 homoplasmic	Apel and Bock, 2009
H.C.	Red Setter	*LCYB*	tomato	Nuclear	T5 homozygous	D'Ambrossio et al., 2004
LCe	IPA6-Lut	*LCYB*	Erwinia	Plastid	T4 homoplasmic	Wurbs et al., 2007

Table S2. Summary of hormones measured by the hormonomics approach in the leaves and fruits of the transgenic *LCYB* lines. Measured hormones (boldfaced); hormones under the detection limit (grey).

Phytohormone group		**#**	**Compound name**	**Abbreviation**
CYTOKININS	BASES, RIBOSIDES	1	*trans*-zeatin	*t*Z
		2	*trans*-zeatin riboside	*t*ZR
		3	*cis*-zeatin	*c*Z
		4	***cis*-zeatin riboside**	***c*ZR**
		5	Dihydrozeatin	DHZ
		6	**dihydrozeatin riboside**	**DHZR**
		7	**Isopentenyladenine**	**iP**
		8	**isopentenyladenine riboside**	**iPR**
	O-GLUCOSIDES	1	*trans*-zeatin-O-glucoside	*t*ZOG
		2	*trans*-zeatin riboside-O-glucoside	*t*ZROG
		3	*cis*-zeatin-O-glucoside	*c*ZOG
		4	***cis*-zeatin riboside-O-glucoside**	**cZROG**
		5	**dihydrozeatin-O-glucoside**	**DHZOG**
		6	**dihydrozeatin riboside-O-glucoside**	**DHZROG**
	N-GLUCOSIDE	1	***trans*-zeatin-7-glucoside**	***t*Z7G**
		2	*trans*-zeatin-9-glucoside	*t*Z9G
		3	***cis*-zeatin-7-glucoside**	***c*Z7G**
		4	***cis*-zeatin-9-glucoside**	***c*Z9G**
		5	**dihydrozeatin-7-glucoside**	**DHZ7G**
		6	dihydrozeatin-9-glucoside	DHZ9G
		7	**isopentenyladenine-7-glucoside**	**iP7G**
		8	isopentenyladenine-9-glucoside	iP9G
2-METHYLTHIO CYTOKININS		1	2-methylthio-isopentenyladenine	2MeSiP
		2	2-methylthio-isopentenyladenine riboside	2MeSiPR

		3	2-methylthio-*cis*-zeatin	2MeS*c*Z
		4	**2-methylthio-*cis*-zeatin riboside**	**2MeS*c*ZR**
AUXINS	PRECURSORS, ACTIVE FORMS	1	**anthranilic acid**	**ANT**
		2	**Tryptophan**	**TRP**
		3	**Tryptamine**	**TRA**
		4	**indol-3-acetamid**	**IAM**
		5	**indol-3-acetic acid**	**IAA**
	CATABOLITE	1	**2-oxoindole-3-acetic acid**	**oxIAA**
	IAA CONJUGATES	1	IAA-glycine	IAA-Gly
		2	IAA-glutamate	IAA-Glu
		3	IAA-alanine	IAA-Ala
		4	IAA-valine	IAA-Val
		5	IAA-leucine	IAA-Leu
		6	IAA-phenylalanine	IAA-Phe
		7	IAA-aspartate	IAA-Asp
JASMONATES		1	**3-oxo-2-(2-(Z)-pentenyl)cyclopentane-1-butyric acid**	**OPC-4**
		2	3-oxo-2-(2-(Z)-pentenyl)cyclopentane-1-hexanoic acid	OPC-6
		3	***cis*-12-oxo-phytodienoic acid**	***cis*OPDA**
		4	**dinor-12-oxo-phytodienoic acid**	**dnOPDA**
		5	**jasmonic acid**	**JA**
		6	11-hydroxy-jasmonic acid	Σ11/12-OH-JA
		7	12-hydroxy-jasmonic acid	
		8	**9,10-dihydrojasmonic acid**	**9,10-dh-JA**
		9	**JA-isoleucine**	**JA-Ile**
		10	JA-valine	JA-Val
		11	JA-phenylalanine	JA-Phe

	12	JA-tryptophan	JA-Trp
SALICYLATES	1	**salicylic acid**	**SA**
ABSCISATES	1	**abscisic acid**	**ABA**
	2	**phaseic acid**	**PA**
	3	**dihydrophaseic acid**	**DPA**
	4	***neo*-phaseic acid**	**NeoPA**
	5	**7-hydroxy-ABA**	**7-OH-ABA**
GIBBERELLINS	1	**Gibberellin 1**	**GA 1**
	2	Gibberellin 3	GA 3
	3	Gibberellin 4	GA 4
	4	Gibberellin 5	GA 5
	5	Gibberellin 6	GA 6
	6	**Gibberellin 8**	**GA 8**
	7	Gibberellin 15	GA 15
	8	**Gibberellin 19**	**GA 19**
	9	Gibberellin 24	GA 24
	10	Gibberellin 29	GA 29
	11	**Gibberellin 34**	**GA 34**
	12	Gibberellin 44	GA 44
	13	Gibberellin 53	GA 53
BRASSINOSTEROIDS	1	Brassinolide	BL
	2	24-*epi*brassinolide	epiBL
	3	Homobrassinolide	homoBL
	4	Castasterone	CS
	5	24-*epi*castasterone	epiCS
	6	Homocastasteron	homoCS
	7	Dolichosterone	DS

	8	Homodolichosterone	homoDS
	9	Teasterone	TE
	10	Typhasterol	TY

Table S3. The SRM transitions of gibberellins detected from tomato tissues.

Analytes	**Retention time (min)**	**Precursor Ion (*m/z*)**	**Product Ion (*m/z*)**	**Collision Energy (V)**	**I.S.**
GA1	4.1	347.2	259.1	20	D_2-GA1
D_2-GA1	4.1	349.2	261.1	20	-
GA3	4.0	345.1	239.1	20	D_2-GA3
D_2-GA3	4.0	347.2	241.1	20	-
GA4	7.6	331.2	257.1	25	D_2-GA4
D_2-GA4	7.6	333.2	259.1	25	-
GA8	2.6	363.1	275.1	20	D_2-GA4
GA9	9.2	315.2	271.0	25	D_2-GA9
D_2-GA9	9.2	317.2	273.0	25	-
GA12	9.9	331.2	313.1	30	D_2-GA12
D_2-GA12	9.9	333.2	315.1	30	-
GA13	5.6	377.2	359.0	20	D_2-GA4
GA19	5.7	361.1	273.1	30	D_2-GA12
GA24	8.0	345.2	257.1	30	D_2-GA9

Table S4. Summary of phenotypic and molecular changes in the leaves/shoot of the transgenic LCYB tomato lines.

Parameter	Phenotype	Transgenic lines		
		pNLyc#2	H.C.	LCe
Plant physiology	Plant height	increased	decreased	increased
	Leaf number	n.c.	decreased	n.c.
	Internode length	increased	decreased	increased
	Days to flowering	increased	decreased	n.c.
Photosynthesis	Conductance	decreased	increased	increased
	ETR	n.c.	increased	n.c.
	ΦPSII	increased	increased	increased
	CO_2 assimilation	n.c.	increased	n.c.
Carotenoids	β-carotene	n.c.	decreased	decreased
	Xanthophylls	increased	increased	decreased
Apocarotenoids	β-cyclocitral	decreased	decreased	decreased
	Zaxinone	decreased	decreased	n.c.
	β-ionone	n.c.	n.c.	n.c.
Phytohormones	ABA	increased	decreased	decreased
	PA	n.c.	n.c.	n.c.
	SA	n.c.	n.c.	n.c.
	iP	n.c.	n.c.	n.c.
	GA1	n.c.	increased	decreased
	GA4	< LOD	< LOD	< LOD
	IAA	n.c.	increased	n.c.
	JA	increased	n.c.	increased
	JA-Ile	< LOD	< LOD	increased

Primary metabolites	Trehalose	increased	decreased	n.c.
	Fructose	increased	n.c.	decreased
	Glucose	n.c.	decreased	n.c.
	Myo-inositol	increased	decreased	increased
	Erythritol	n.c.	increased	n.c.
	Putrescine	increased	decreased	increased
	Val	increased	decreased	n.c.
	Asp	n.c.	n.c.	increased
	Asn	increased	decreased	n.c.
	Glu	n.c.	decreased	n.c.
	Gln	increased	decreased	increased
	Ala	increased	decreased	increased
Stress tolerance	High light	increased	increased	n.c.
	Drought	increased	increased	increased
	Salt	increased	increased	increased

*<LOD: below limit of detection; n.c.: not changed; H.C.: high carotene; LCe: lycopene β-cyclase from Erwinia.

Table S5. Summary of phenotypic and molecular changes in the fruits of the transgenic LCYB tomato lines.

Parameter	Phenotype	pNLyc#2	H.C.	LCe
Fruit physiology	Fruit number	decreased	increased	n.c.
	Fruit size	n.c.	increased	increased
Plant biomass and yield	Fruit biomass	decreased	increased	increased
	Seed yield	decreased	increased	decreased
Carotenoids	β-carotene	increased	increased	increased
	Xanthophylls	decreased	decreased	n.d.
Apocarotenoids	β-cyclocitral	increased	increased	decreased
	Zaxinone	n.c.	decreased	increased
	β-ionone	increased	increased	n.c.
Phytohormones	ABA	increased	increased	n.c.
	PA	increased	decreased	n.c.
	SA	increased	n.c.	n.c.
	iP	increased	decreased	increased
	GA1	< LOD	< LOD	< LOD
	GA4	< LOD	< LOD	< LOD
	IAA	decreased	decreased	increased
	JA	increased	increased	n.c.
	JA-Ile	increased	increased	n.c.
Primary metabolites	Trehalose	n.c.	increased	decreased
	Fructose	n.c.	increased	n.c.
	Glucose	increased	n.c.	Increased
	Myo-inositol	decreased	increased	decreased
	Erythritol	decreased	increased	decreased

	Putrescine	n.c.	increased	increased
	Val	increased	n.c.	n.c.
	Asp	increased	increased	n.c.
	Asn	increased	decreased	increased
	Glu	increased	increased	n.c.
	Gln	increased	n.c.	n.c.
	Ala	increased	n.c.	n.c.
Shelf life	Shelf life	increased	increased	increased

*<LOD: below limit of detection; n.c.: not changed; n.d.: not detected; H.C.: high carotene; LCe: lycopene β-cyclase from Erwinia.

Table S6. The SRM transition list for apocarotenoid profiling.

No.	ID	RT	Precursor ions	Product ions
		(min)	*m/z* $[M+H]^+$	*m/z* $[M+H]^+$
1	β-Cyclocitral	7.4	153.1	109.1
2	β-Ionone	9	193.2	175.1
3	β-Apo-11-carotenal	10	219.2	163.1
4	β-Apo-13-carotenone	11	259.2	175.1
5	β-Apo-15-carotenal	11.8	285.2	175.1
6	β-Apo-14'-carotenal	12.6	311.2	119.1
7	β-Apo-12'-carotenal	14.1	351.3	119.1
8	β-Apo-10'-carotenal	14.5	377.3	119.1
9	β-Apo-8'-carotenal	15.8	417.3	119.1
10	3-OH-β-ionone	5.5	209.2	109.1
11	3-OH-β-apo-11-carotenal	6.3	235.2	217.1
12	3-OH-β-apo-13-carotenone	7.2	275.2	173.1
13	3-OH-β-apo-15-carotenal	8	301.2	173.1
14	3-OH-β-apo-14'-carotenal	8.7	327.2	173.1
15	3-OH-β-apo-12'-carotenal	9.9	367.3	161.1
16	3-OH-β-apo-10'-carotenal	10.1	393.3	119.1
17	3-OH-β-apo-8'-carotenal	11	433.3	161.1
18	D_3-β-Ionone	9	196.2	178.2
19	D_3-β-Apo-11-carotenal	10	222.2	163.1
20	D_3-β-Apo-13-carotenone	11	262.2	178.2
21	D_3-β-Apo-15-carotenal	11.8	288.2	178.2
22	D_3-β-Apo-14'-carotenal	12.6	314.2	119.1
23	D_3-β-Apo-12'-carotenal	14.1	354.3	119.1
24	D_3-β-Apo-10'-carotenal	14.5	380.3	119.1
25	D_3-β-Apo-8'-carotenal	15.8	420.3	119.1
26	D_3-3-OH-β-apo-13-carotenone	7.2	278.2	176.2